Original article

Preparation and in vivo evaluation of nano sized cubosomal dispersion loaded with Ruta graveolens extracts as a novel approach to reduce asthma-mediated lung inflammation

Mohammad H. Alyami [a], Dalia I. Hamdan [b], Heba M.A. Khalil [c,*], Mohamed A.A. Orabi [d,e], Nora M. Aborehab [f], Nada Osama [g], Mai M. Abdelhafez [h], Abdulaziz Mohsen Al-Mahallawi [i], Hamad S. Alyami [a,*]

[a] Department of Pharmaceutics, College of Pharmacy, Najran University, Najran 66462, Saudi Arabia
[b] Department of Pharmacognosy and Natural Products, Faculty of Pharmacy, Menoufia University, Shibin Elkom 32511, Egypt
[c] Department of Veterinary Hygiene and Management, Faculty of Veterinary Medicine, Cairo University, Giza 12211, Egypt
[d] Department of Pharmacognosy, College of Pharmacy, Najran University, Najran, Saudi Arabia
[e] Department of Pharmacognosy, Faculty of Pharmacy, Al-Azhar University, Assiut-branch, Assiut 71524, Egypt
[f] Department of Biochemistry, Faculty of Pharmacy, October University for Modern Sciences and Arts (MSA), Giza 12451, Egypt
[g] Biochemistry Department, Faculty of Pharmacy, Menoufia University, Gamal Abd El Nasr st., Shibin Elkom, 32511 Menoufia, Egypt
[h] Department of Pharmacology and Toxicology, Faculty of Pharmacy, MSA University, Egypt
[i] Department of Pharmaceutics and Industrial Pharmacy, Faculty of Pharmacy, Cairo University, Cairo, Egypt

ARTICLE INFO

ABSTRACT

Asthma is a chronic disease affecting people of all ages. Asthma medications are associated with adverse effects restricting their long-term usage, demanding newer alternative therapies. This study aimed to investigate the anti-asthmatic properties of *Ruta graveolens* extract and its prepared nano-cubosomal dispersion (Ruta-ND). Firstly, the *R. graveolens* methanolic extract exhibited higher anti-inflammatory activity on Lipopolysaccharide (LPS)-activated BEAS-2B cells. To ensure best bioavailability and hence best cellular uptake, *R. graveolens* extract was loaded in nano-cubosomal dispersion (ND). Then, the anti-asthmatic effects of *Ruta* extract and ND were simultaneously evaluated in rats' model with ovalbumin-induced allergic asthma. *R. graveolens* extract and Ruta-ND subsided asthma score and improved lung function by restoring FEV1/FVC ratio to the expected values in control rats. Also, it showed strong antioxidant and anti-inflammatory activities manifested by lowering levels of malondialdehyde (MDA), IL-4, IL-7, TGF-β, and Ig-E, and increasing levels of superoxide dismutase (SOD) and INF-γ in bronchoalveolar lavage fluid. Our research findings also indicate autophagy induction and apoptosis inhibition by *Ruta* extract and Ruta-ND. Finally, the HPLC MS/MS phytochemical profiling of *R. graveolens* extract evident production of various alkaloids, flavonoids, coumarins, and other phenolics with reported pharmacological properties corresponding to/emphasize our study findings. In conclusion, *R. graveolens* exhibited promise in managing Ova-induced allergic asthma and could be developed as an alternative anti-allergic asthma drug.

1. Introduction

Asthma is a complex disease of the airways, affecting nearly 300 million people worldwide. It is characterized by chronic airway inflammation, bronchial hyper-reactivity, excessive mucus production, airway wall remodeling, and constriction (Nelson, 2001; Dharmage et al., 2019). It is one of the most common chronic diseases affecting children (Poole, 2014). In the Middle East, the overall prevalence of asthma in children accounts for 10–30 %, with the highest occurrence in Saudi Arabia (23 %) (Hasnain, 2016). Loss of Type 1 T helper (Th1)/Type 2 T helper (Th2) cells equilibrium is considered a key player in the etiology of asthma (Packard and Khan, 2003). Changes in interferon-

gamma (IFN-γ) and interleukin-4 (IL-4) levels released by Th1 and Th2 cells can cause a Th1/Th2 imbalance (Hasnain, 2016). Some research suggests that the pathophysiology of asthma may also involve a breakdown of balance between regulatory T cells (Treg) and Th17 cells (Tao, 2015). Where, Interleukin-17 (IL-17), produced by activated Th17, controls pulmonary inflammation in airway smooth muscle cells and fibroblasts (Schnyder-Candrian, 2006), also, the regulatory T cells secrete transforming growth factor beta (TGF-β) and Interleukin-10 (IL-10), which may cause immunological suppression. And this will lead to the presence of levels of IL-17, TGF-β, and IL-10 during the start of asthma are reliable indicators of the presence of Th17 and Treg cells (Hou et al., 2016).

Another mechanism involved in asthma pathogenesis is dysregulated autophagy, with opposing effects showing both harmful and beneficial consequences (Zeki, 2016; Racanelli, 2018; Painter et al., 2020). Autophagy is a cellular mechanism that maintains cell survival by removing dysfunctional organelles or proteins. It associates with inflammatory responses due to lung infection, stress, and asthma (Jiang et al., 2017; Racanelli, 2018).

Beclin 1 is one of the first-described mammalian autophagy protein (Liang et al., 1998). Beclin 1 is a positive regulator of autophagy (Liang et al., 1999) and a key component of a Class III PI3K complex involved in the initiation of autophagosome formation (Yue and Zhong, 2010).

On the other hand, p62 protein, an autophagy marker, is degraded by autolysosomes following the initiation of autophagy. As a result, the buildup of p62 has been recognized as a general indicator of decreased autophagic flux (Yoshii and Mizushima, 2017).

Like autophagy, dysregulation of apoptosis may be involved in asthma pathogenesis. The development of asthma as well as its clinical severity may be directly influenced by changes in the apoptosis of both mobile and resident cells of the airways (Cryns and Yuan, 1998; Vignola, 2000; Duncan, 2003; Spinozzi et al., 2008). Both the intrinsic and extrinsic pathways of apoptosis activate caspases, which are cysteine proteases that are central regulators of apoptosis. Caspase 3 is one of the most frequently activated proteases involved in apoptosis (Abbas et al., 2019). It is considered the key executor of caspase in apoptosis (Zhou, 2011; Nadeem, 2015). The level of apoptotic caspase 3 protein was found to be increased in bronchial epithelial cells or lung tissues in asthma (Enari et al., 1998; Jang et al., 2014).

Moving to asthma treatment, systemic corticosteroids and β 2-agonists are common asthma therapies (Mukherjee and Zhang, 2011). These medications have powerful benefits when used alone or in combination but also have adverse side effects that restrict their long-term use (Papiris et al., 2009). Therefore, it is essential to create alternative compounds with comparable therapeutic potential and fewer side effects to manage airway illnesses. Natural products have several benefits, including low cost, biocompatibility, fewer adverse effects, and extensive biodiversity and renewability, drawn wide researcher interest as asthma replacement therapy (Biavatti, 2007; Huntley and Ernst, 2000).

Several plant members of the Rutaceae family are utilized in alternative medicine worldwide. *Ruta graveolens* L (*R. graveolens*), known as "Ruta" is the most prevalent plant. It has primarily been utilized for gastrointestinal diseases, respiratory illnesses, and menstrual problems in folk medicine (Miguel and Rue, 2003; Pollio et al., 2008). Also, it has been cited in several scientific publications for its anti-inflammatory (Raghav et al., 2007), sperm motility-inhibitory (Harat et al., 2008), algicidal and antifungal (Meepagala et al., 2005), antibacterial (Ojala et al., 2000), and even anti-carcinogenic (Preethi et al., 2006), and antioxidant effects (Ratheesh et al., 2009; Ratheesh, 2011).

Ruta graveolens has a potent anti-inflammatory and antioxidant properties due to the presence of bioactive substances including the highly, if not the most, abundant flavonoids quercetin and rutin (Colucci-D'Amato and Cimaglia, 2020).

Although their wider acceptability as saver substitute of synthetic drugs, the phyto-molecules have some restrictions, such as limited absorption, decreased bioavailability, and efficacy. Loading the phyto-molecules into nanostructures is one of the promising techniques to enhance their efficacy through decreasing the needed dosage, increasing the solubility, and consequently enhancing the bioavailability and improving their cellular uptake and biodistribution for better-targeting behavior (Gera et al., 2017). Different types of lipid-based nano-systems have been developed to improve the *in-vivo* performance of herbal drugs. Among these, nano-cubosomes are potential carriers owing to their great potential as a promising delivery system compared to the traditional lipid vesicles, liposomes. Nano-cubosomal dispersion (ND), especially those composed of binary systems of glyceryl monooleate (GMO) and water, are the most tested systems (Farag et al., 2022). These systems are considered hydrophilic surfactant-containing systems that exhibit the ability to self-assemble as a bicontinuous cubic liquid crystalline phase (Bei et al., 2009). ND are distinguished by their viscous texture, high surface area, and large ability to be loaded with hydrophilic, lipophilic, and amphiphilic drugs (Nylander et al., 1996). Furthermore, these nano-cubosomal systems are biocompatible, bioadhesive, and biodegradable (Al-Mahallawi et al., 2021).

In this study, dried powdered herb of *R. graveolens* was extracted by homogenization in MeOH to obtain total extract (TE). The fractions (EtOAc-Fr), methanol (MeOH-Fr), and butanol fractions (But. Fr) were obtained by flash chromatography from the total extract by the corresponding solvents. Then part of the TE was prepared as nano-cubosomal dispersion (Ruta-ND. The objectives of this study are to investigate the *in-vitro* anti-inflammatory properties of the *R. graveolens* total extract (TE) and different fractions EtOAc-Fr, MeOH-Fr, and But-Fr, as well as the prepared Ruta-ND, and to explore the underlying mechanism of the most active TE and Ruta-ND in inhibiting apoptosis, oxidative stress, and inflammation via modulation of different signaling pathways in asthmatic rat model sensitized to ovalbumin (Ova). *R. graveolens*' TE was also subjected to an ultra-high performance liquid chromatography electrospray ionization mass/mass (UPLC-ESI-MS/MS) extensive metabolites profiling in order to investigate its phytochemicals that underpin these anti-asthmatic activities.

2. Materials and methods

2.1. Plant material

Fresh herbal plants in the early flowering stage of *R. graveolens* L., were purchased from an ornamental garden in Najran city, Kingdom of Saudi Arabia (KSA). A voucher specimen (Rg-102021) was kept at the College of Pharmacy, Najran University, KSA. The aerial parts were dried in the shade, and the leaves and young stem branches were crushed into fine powder by a milling machine, then submitted to solvent extraction as follows:

2.2. Preparation of the plant extract and fractions

A total of 0.5 kg of dried leaves were extracted by MeOH (4 × 2 L) using a homogenizer. The total extract (TE) was dried under reduced pressure until reached a constant weight (168 g). A portion (31 g) of the total extract was kept for further studies. The majority (137 g) of the dried total extract was then slurred with silica gel and subjected to flash chromatography on a silica gel column (40 × 10 cm, i.d) using hexane (3 L), EtOAc (4 L), butanol (4 L), and MeOH (3 L), successively. The collected different eluates were dried under reduced pressure to obtain the corresponding hexane (20 mg), EtOAc (20.3 g), butanol (21 g), and MeOH (95 g) fractions, which were kept in dry amber bottles for performing chemical and biological studies.

2.3. In-vitro study

2.3.1. Cell culture

The human non-tumorigenic lung epithelial (BEAS-2B) cells, were supplied by VACSERA (Giza, Egypt). The cells were cultured in
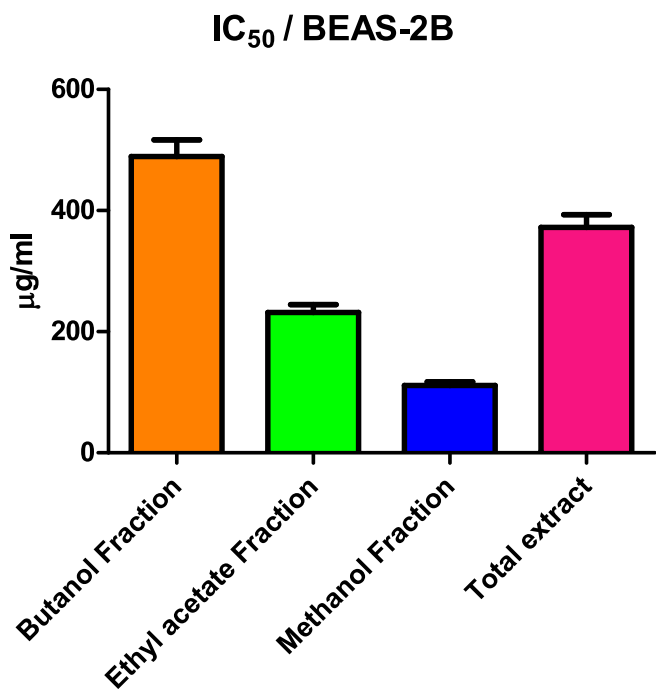
IC$_{50}$ / BEAS-2B

Fig. 1. IC$_{50}$ of butanol fraction (But), ethyl acetate fraction (EtOAc), methanol fraction (MeOH), and TE of *R. Graveolens* on BEAS-2B cells.

Dulbecco's Modified Eagle Medium (DMEM) medium (Invitrogen/Life Technologies) supplemented with 10 % fetal bovine serum (Hyclone), 10 µg/ml of insulin [Sigma Aldrich, United States of America (USA)], 1 % penicillin and 1 % streptomycin (Sigma Aldrich, USA) at 37 °C under an atmosphere of 5 % CO_2 and 95 % air.

2.3.2. Growth inhibition assay

The growth inhibitory effects of serial dilution of TE, as well as the different fractions (EtOAc, MeOH, and Butanol) (1000, 250, 63,16,4 µg/ml) were detected by 3-(4,5-dimethylthiazol-2-yl)-2,5-diphenylte-trazolium bromide dye (MTT) assay (Han and Park, 2009). BEAS-2B cells were cultured in 96-well plates at a density of 1×10^5 cells/well and incubated at 37 °C for 24 h to form a complete monolayer sheet. The cells were treated individually with serial dilution of the four extracts and incubated for 48 h. The morphology changes were observed under inverted microscopy & MTT solution was added to each well of 96-well plate. The plate was incubated for 4 h at 37 °C & 5 % CO_2. After incubation, MTT solubilization solution [M−8910] was added in equal amounts to the volume of the original culture medium to solubilize the formazan crystals. Absorbance was measured spectrophotometrically at 570 nm, and the value was determined in comparison to control cells. Effect of the four extracts on BEAS-2B cells proliferation were evaluated by the calculation of cell viability (%) and IC$_{50}$ (the concentration of the drug required to kill 50 % of cells relative to the untreated cultures) of each extract.

2.3.3. Lipopolysaccharide (LPS) activation of BEAS-2B cells

BEAS-2B cells were treated with IC$_{50}$ and ½ IC$_{50}$ of the four different extracts for 2 h, and then stimulated with 2 µg/mL LPS for 8 h (Kim et al., 2017). The control was performed using cells treated with LPS only. After incubation, total RNA was extracted using the RNeasy mini kit (Qiagen, GmbH, Germany) according to the manufacturer's protocol.

2.3.4. Reverse transcription-polymerase chain reaction (RT-PCR)

Primers for interleukin (IL)-17, transforming growth factor-beta (TGF-β), IL-4, interferon gamma (IFN-γ), and housekeeping gene
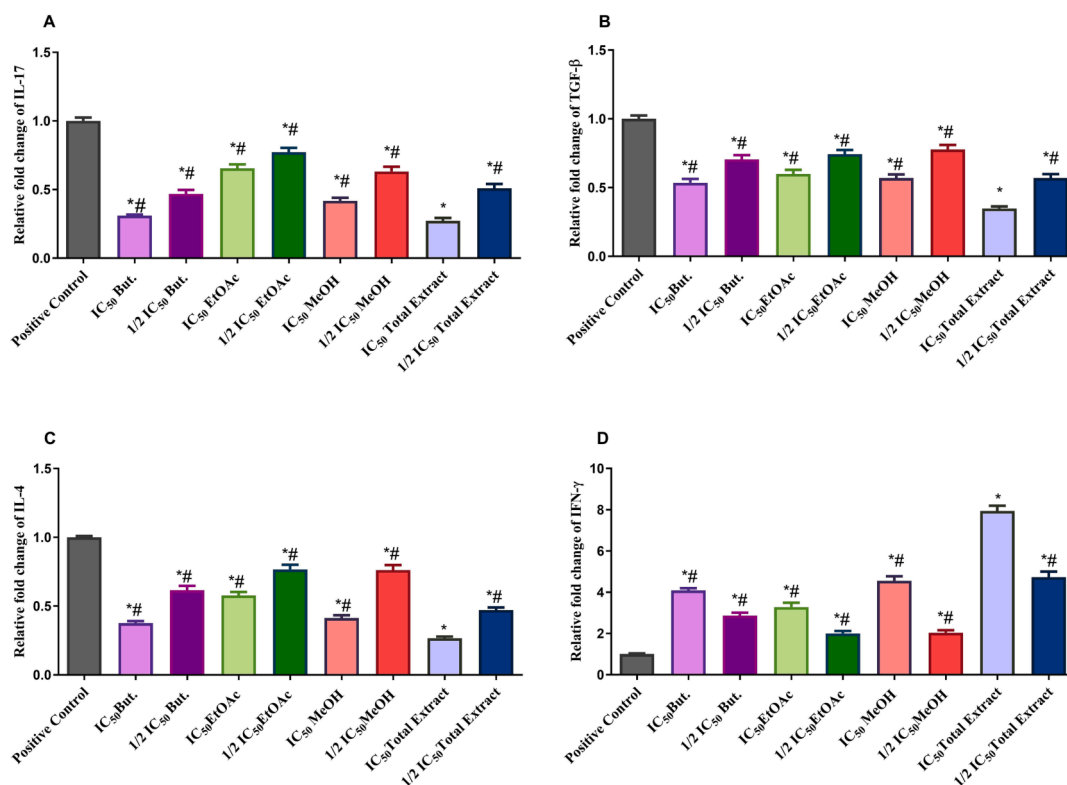

Fig. 2. Real-time PCR analysis data depicting the relative normalized expression of IL-17, IL-4, TGF-β, and IFN-γ after BEAS-2B treatment with IC$_{50}$ and ½ IC$_{50}$ of But., EtOAc, MeOH, and TE of *R. graveolens*. P-values on the graph reflect the statistical significance of various treatments compared to positive control (stimulated with LPS). The relative expression was calculated based on the $2 − \Delta\Delta Ct$ method. * Significance from positive control at $P < 0.0001$, # Significance from IC$_{50}$ of TE treatment at $P < 0.0001$.
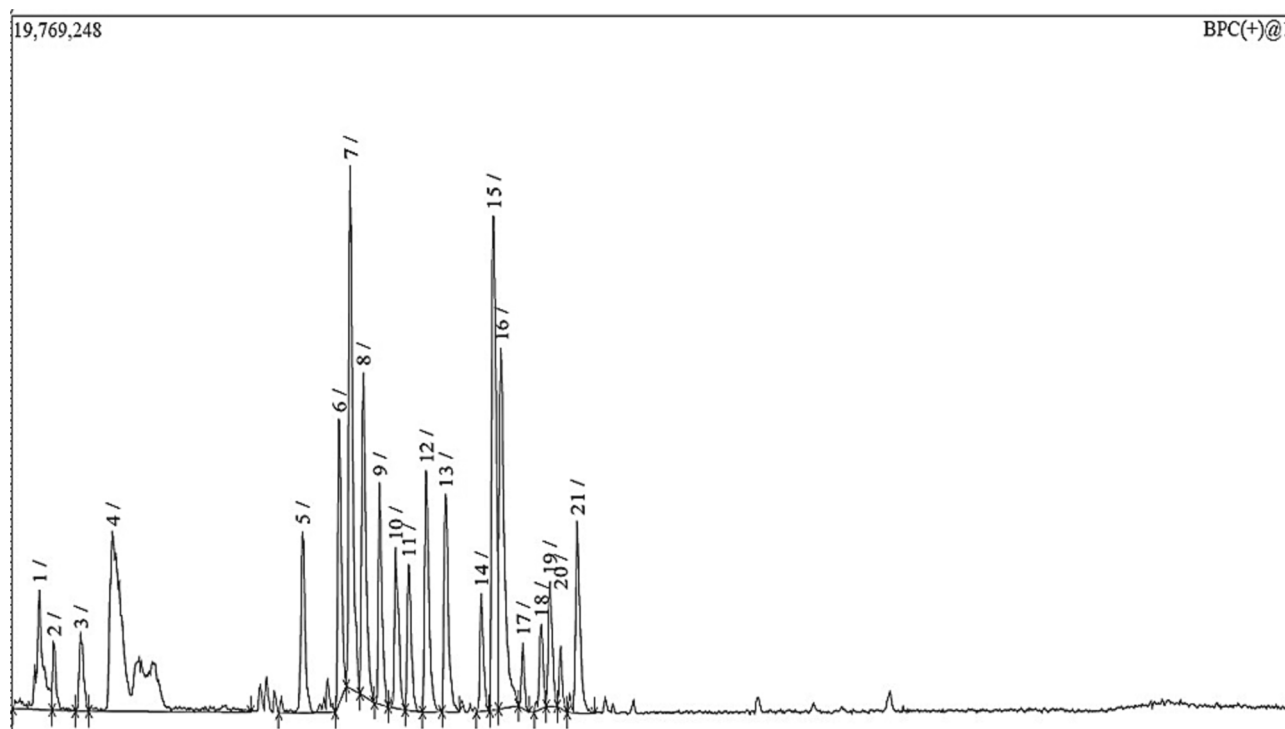
Fig. 3. HPLC-PDA-ESI-MS/MS chromatogram (positive ionization mode) of total MeOH extract of *R. graveolens.*

"β-actin" were purchased from Thermo Fisher Scientific Inc., Germany (Table S1). RT-qPCR was carried out using the iScript TM One-Step RT-PCR Kit with SYBR® Green (Bio-Rad Laboratories, California, United States) following manufacturer's instructions. All values are shown after normalization to a β-actin control. Finally, values were shown as fold changes using the following equation: $2^{\hat{}}\Delta\Delta CT$.

2.4. Preparation of R. graveolens extract-loaded nano-cubosomal dispersion (Ruta-ND)

2.4.1. Experimental procedures

Ruta-ND was prepared by the hot emulsification method previously reported by Al-Mahallawi et al. (2021) (Al-Mahallawi et al., 2021) with minor adjustments. In brief, GMO (Sigma-Aldrich Co., St. Louis, MO, USA) was accurately weighed into a glass vial and allowed to melt at 70 °C on a hot plate. Then Ruta TE extract was dispersed in the molten lipid at the same temperature. Afterward, the lipid phase was slowly emulsified into previously heated aqueous phase containing Pluronic F1018 (Sigma-Aldrich Co., St. Louis, MO, USA), which acts as a stabilizer. The obtained dispersion was allowed to cool gradually to room temperature. The formed Ruta-ND was kept in glass vials at 2–8 °C for further studies. The final concentrations of GMO, Pluronic F108, Ruta extract, and deionized water were 4, 1, 4.5, and 90.5 % w/w, respectively. It is worth mentioning that the chosen nano-cubosaomal system was based on preliminary trials (data not shown).

2.4.2. Characterization of Ruta-ND

The particle size (PS) and polydispersity index (PDI) of Ruta-ND were measured using Zetasizer Nano ZS (Ver.6.12, Malvern Instruments Ltd., Worcestershire, England) utilizing the dynamic light scattering technique at room temperature (El Said et al., 2022). Also, the zeta potential (ZP) of the prepared Ruta-ND was determined using the same equipment at room temperature (Fahmy et al., 2021). The dispersion was appropriately diluted with deionized water before any measurement. All measurements were performed in triplicates (Albash et al., 2021). Moreover, the morphology of the nano-cubosomal system was assessed

using transmission electron microscopy (TEM) (Joel JEM 1230, Tokyo, Japan). A copper grid was loaded with the diluted dispersion which was subjected to negative staining with aqueous solution of phosphotungstic acid (2 % w/v) for a duration of 5 min. Drying of the grid at ambient temperature for 10 min was then followed prior to visualization under a transmission electron microscope.

2.5. In-vivo evaluation of the anti-asthmatic activity of Ruta-ND

2.5.1. Ova administration

The Ova was obtained from the Sigma-Aldrich Chemical Company. It was used to induce the asthma model as previously described (Sakat et al., 2018). Briefly, 0.3 mg Ova and 30 mg aluminum hydroxide [Al (OH)$_3$] were dissolved in a saline solution. This mixture was administered by the intraperitoneal (IP) route from day one to day four and then on day 11th (five doses were thus administered). Following this sensitization stage, the challenge was applied once daily for three days between days 19 and 21. Rats were administrated with a volume of 20 μl of 20 mg/ml Ova solution dissolved in 1 ml saline solution intranasally using a micropipette.

2.5.2. Animal and experimental design

Male Wistar rats (n = 42) weighing 150–200 g were purchased from a commercial breeding unit (Giza, Egypt). Rats were adapted in plastic cages for seven days under standard climatic conditions that were maintained throughout the experiment. The experimental design was approved by the institutional animal care and use committee of the Faculty of Veterinary Medicine (Vet-IACUC, Approval number: Vet CU 03162023707), Cairo University. Also, it conducted in accordance with EU Directive 2010/63/EU for animal experiments. Then, the adapted rats were randomly divided into six groups:

- Group 1 (Control group). Rats without sensitization or challenge and a 2 ml/kg dose of saline solution were administered at the challenge stage by oral gavage.

Table 1

Metabolites identified from the total MeOH extract of *R. graveolens*.

Identification	Molecular formula	Rt (min)	*m/z*	MS/MS fragments
Methyl cnidioside A	$C_{18}H_{22}O_9$	0.95	383.01	369,284, 207, 122
Daphnoretin methyl ether	$C_{20}H_{14}O_7$	1.67	367.1	353, 339, 194, 116
1,4-Dihydro-4-methoxy-1,4-dimethyl-3-(3-methylbut-2-enyl) quinoline-2,7-diol	$C_{17}H_{23}NO_3$	2.75	290.01	221, 207, 177, 163
Epicatechin	$C_{15}H_{14}O_6$	2.78	291.01	247, 207, 181
Umbelliferone	$C_9H_6O_3$	2.85	163.01	147, 135, 119
Rutacultin	$C_{16}H_{18}O_4$	3.82	275.01	260, 232, 220
Vecenin-2	$C_{27}H_{30}O_{15}$	5.19	595.1	505, 475, 415
Pinnarin	$C_{16}H_{18}O_4$	5.83	275.01	260, 232, 220
Rutaretin	$C_{14}H_{14}O_5$	6.57	263.01	205, 189, 161
Gossypetin 7-methyl ether 3-rutinoside	$C_{28}H_{32}O_{17}$	6.63	641.1	495, 333, 303
Gossypetin methyl ether	$C_{16}H_{12}O_8$	6.67	333.1	303
Rutin	$C_{27}H_{30}O_{16}$	6.77	611.01	465, 303
Quercetin 3-rhamnoside (Quercitrin)	$C_{21}H_{20}O_{11}$	6.8	449.01	303
Isoquercitrin, quercetin-3-O-b-D-glucopyranoside	$C_{21}H_{20}O_{12}$	6.81	465.01	303
Quercetin	$C_{15}H_{10}O_7$	6.97	303.01	153, 108
Isorhamnetin 3-O-Rutinoside	$C_{28}H_{32}O_{16}$	7.24	625.1	317, 301
Cnidioside A	$C_{17}H_{20}O_9$	7.37	369.1	284, 207, 122
4-Hydroxy-2-undecylquinoline	$C_{20}H_{29}NO$	7.77	300.01	198, 184, 172
Bergapten	$C_{12}H_8O_4$	7.81	217.01	161, 131
Graveoline	$C_{17}H_{13}NO_3$	8.01	280.01	266, 237, 207
Graveolinine	$C_{17}H_{13}NO_3$	9.01	280.01	266, 251, 223
Skimmianine, Kokusaginin (4,6,7-Trimethoxyfuro [2,3-b] quinoline)	$C_{14}H_{13}NO_4$	9.25	260.01	245, 230, 216, 199, 184
Rutacridone	$C_{19}H_{17}NO_3$	9.38	308.01	294, 253
Psoralen	$C_{11}H_6O_3$	9.41	187.01	159, 143, 131, 115
γ -Fagarine	$C_{13}H_{11}NO_3$	9.61	230.01	215, 201, 157, 129
Rutacridone epoxide	$C_{19}H_{17}NO_4$	10.02	324.01	295, 251
Scopoletin	$C_{10}H_8O_4$	10.12	193.01	178, 150, 132
Dictamnine	$C_{12}H_9NO_2$	10.38	200.01	185, 157, 129
Caffeic acid	$C_9H_8O_4$	10.45	181.01	163, 135
Xanthotoxin, (Methoxsalen; 8-Methoxypsoralen)	$C_{12}H_8O_4$	10.49	217.01	202, 174, 161, 145, 131
Pteleine (6-Methoxydictamnine)	$C_{13}H_{11}NO_3$	10.55	230.01	216, 202, 185, 157
3-(1,1-Dimethylallyl) herniarin	$C_{15}H_{16}O_3$	10.83	245.01	230, 217, 175
2-Heptyl-4(1H)-quinolone	$C_{16}H_{21}NO$	10.85	244.01	215, 186, 145
Syringic acid	$C_9H_{10}O_5$	10.92	199.01	184, 155
4-Hydroxy-2-decylquinoline	$C_{19}H_{27}NO$	11.32	286.01	198, 172, 132
Kaempferol	$C_{15}H_{10}O_6$	11.33	287.01	231, 153, 107
Gravacridonol	$C_{19}H_{17}NO_4$	11.36	324.01	324, 308, 286
(epi) Gallocatechin	$C_{15}H_{14}O_7$	12.29	307.01	263, 221, 181, 167
Chalepin	$C_{19}H_{22}O_4$	13.4	315.01	300, 273, 259, 255, 213, 201
Isorhamnetin	$C_{16}H_{12}O_7$	13.37	317.01	303, 151, 107
Arborinine	$C_{16}H_{15}NO_4$	13.97	286.01	271, 253, 244, 225, 199
1-Methyl-2-nonyl-4(1H)-quinolone	$C_{19}H_{27}NO$	14.44	286.01	186, 159, 173
Luteolin	$C_{15}H_{10}O_6$	14.47	287.01	269, 245201, 153
Apigenin	$C_{15}H_{10}O_5$	14.71	271.01	253, 227, 199, 151
3-Caffeoylquinic acid	$C_{16}H_{18}O_9$	15.04	355.01	193, 181
Rosmarinic acid	$C_{18}H_{16}O_8$	15.07	361.1	199, 181
Gravacridontriol-O-18- β-D-glucoside	$C_{25}H_{29}NO_{11}$	15.31	520.1	358, 267, 253
Chalepensin	$C_{16}H_{14}O_3$	15.44	255.01	199, 171

Table 1 (*continued*)

Identification	Molecular formula	Rt (min)	*m/z*	MS/MS fragments
1-Methyl-2-decyl-4(1H)-quinolone	$C_{20}H_{29}NO$	15.48	300.01	186, 173
Gravacridonetriol	$C_{19}H_{19}NO_6$	16.42	358.1	267, 253
Rutamarin	$C_{21}H_{24}O_5$	16.42	357.01	288, 256, 187
5-Caffeoylquinic acid	$C_{16}H_{18}O_9$	16.75	355.1	193
1-Methyl-2-undecyl-4(1H)-quinolone	$C_{21}H_{31}NO$	17.02	314.01	295, 272, 228, 186, 173
Gravelliferone	$C_{19}H_{22}O_3$	17.55	299.01	231, 215, 171
1-Methyl-2-dodecyl-4(1H)-quinolone	$C_{22}H_{33}NO$	17.82	328.01	315, 283, 255, 221, 186, 173, 152
Daphnoretin	$C_{19}H_{12}O_7$	18.43	353.01	339, 194, 116
Gravacridonediol	$C_{19}H_{19}NO_5$	19.77	342.01	267, 253
4-Caffeoylquinic acid	$C_{16}H_{18}O_9$	20.27	355.01	193, 175

- Group 2 (Ova group): Rats were sensitized with Ova, and a 2 ml/kg dose of saline solution was administered at the challenge stage by oral gavage.
- Group 3 (Ruta 100 mg): Rats were treated with TE of *R. graveolens* (100 mg/kg).
- Group 4 (Ruta 200 mg): Rats were treated with TE of *R. graveolens* (200 mg/kg).
- Group 5 (Ruta-ND 100 mg): Rats were treated with Ruta-ND (100 mg/kg).
- Group 6 (Ruta-ND 200 mg): Rats were treated with Ruta-ND (200 mg/kg).
- Sensitization and challenge were applied with Ova to all groups except control group. All the corresponding treatments were administrated once daily by oral gavage for 10 days starting from day 12th post sensitization and continued till the last three days of the challenge.

2.5.3. Behavioral assessment

After the last challenge dose, rats were subjected to behavioral scoring for 3 min and scored according to the number of itching, sneezing frequency, and degree of the runny nose (Ma et al., 2014). The sum of these three symptom scores were calculated.

2.5.4. Respiratory function measurements

For lung function measurements, a plethysmograph has been used. Rats were placed in the body of plethysmograph, while the nose is projected from a latex into small chamber. The respiration rate was detected through pressure changes in the chamber and recorded via a spirometer with an MTL1 flow meter and AID instruments® Power Lab, with lab chart 8 for analysis. The following parameters were measured: Forced vital capacity (FVC), Forced expiratory volume in the first second (FEV1), and the FEV1/FVC ratio.

2.5.5. Biochemical analysis

After measuring the respiratory functions, rats were subjected to cervical dislocation, and the chest was exposed to visualize the lungs. Then, the tracheae were cannulated, and the airway lumina was washed with 3×2 ml of saline solution. The liquid bronchoalveolar lavage fluid (BALF) was collected and centrifuged at 400 g for 10 min. The supernatant was collected and stored at − 80 ℃ until assayed. Lung tissue was isolated from each rat, first part of lung tissue was homogenized in lysis buffer (50 mM Tris-HCl with 2 mM EDTA, pH 7.4), then after homogenization, the samples were centrifuged for 20 min. at 20,000 rpm, the supernatant was separated and stored at − 80 ℃ until assayed, and the second part of lung tissue was preserved in neutral buffer formalin 10 % for histopathological and immunohistochemical examination.

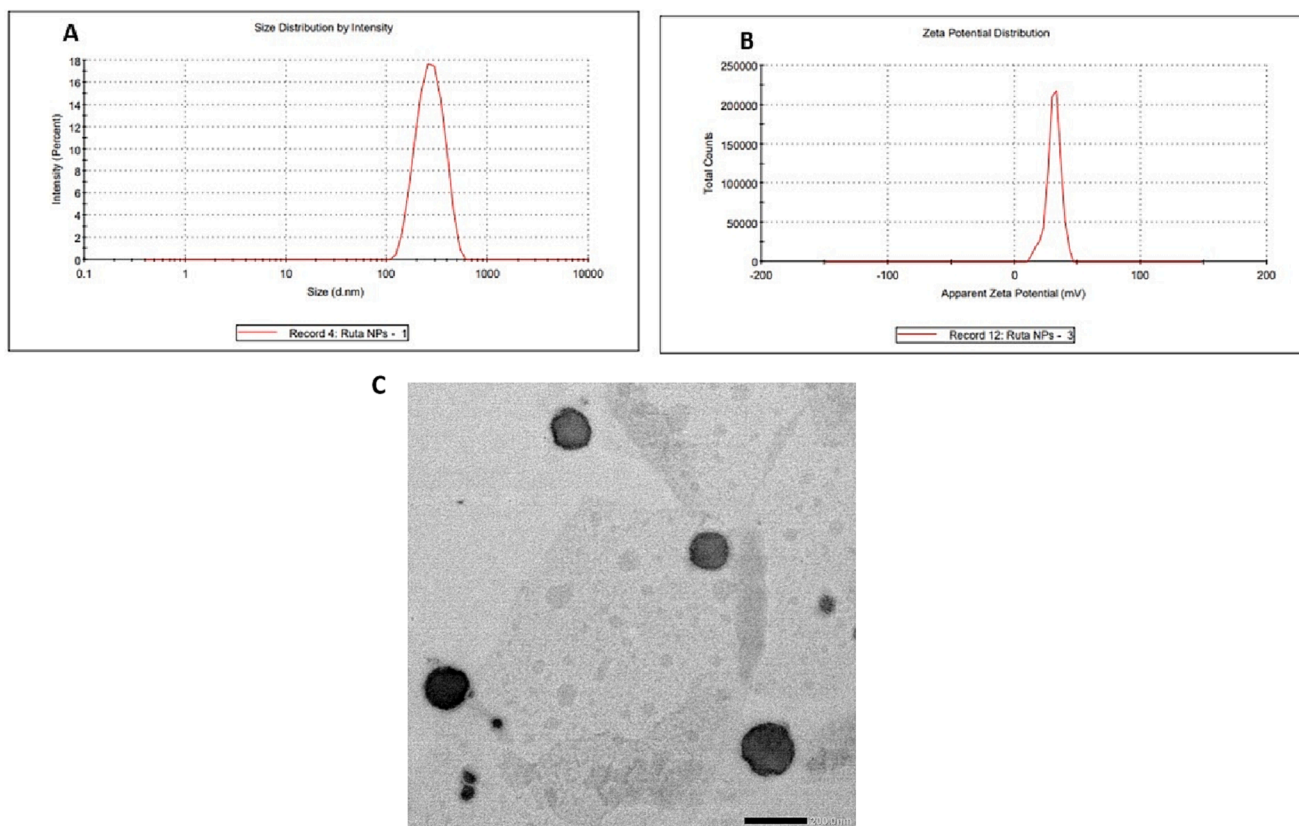- Measurement of oxidative stress biomarkers

Fig. 4. (A). Size distribution, (B). Zeta potential (ZP) of Ruta-ND, and (C). Transmission electron micrograph of the nano- cubosomal system.

Table 2
Behavioral scoring in the different experimental groups.

Groups	Itching frequency (number of times)	Sneezing frequency (number of times)	Runny nose frequency (number of times)
Control	0.20 ± 0.31	0.10 ± 0.05	0.12 ± 0.01
Ovalbumin	5.4 ± 0.04	5.6 ± 0.03	6.0 ± 0.1
Ruta 100 mg	$1.2 \pm 0.2^*$	$1.5 \pm 0.2^*$	$1.5 \pm 0.10^*$
Ruta 200 mg	$0.89 \pm 0.30^{\#}$	$0.70 \pm 0.20^{\#}$	$0.75 \pm 0.30^{\#}$
Ruta-ND 100 mg	$0.63 \pm 0.12^{\#}$	$0.60 \pm 0.20^{\#}$	$5.9 \pm 0.2^{\#}$
Ruta-ND 200 mg	$0.30 \pm 0.01^{\#}$	$0.29 \pm 0.40^{\#}$	$0.5 \pm 0.1^{\#}$

Data expressed as mean $\pm$ standard deviation using one-way ANOVA followed by Tuckey *post hoc* test. * compared to control, # compared to Ova group.

The concentration of MDA and SOD (Biodiagnostic, Diagnostic, and Research Reagents, Egypt) were determined in BALF calorimetrically by an ultraviolet (UV)/Visible spectrophotometer (Shimadzu spectrophotometer 2401 UV/Visible, Japan).

- Measurement of INF-γ, IL-4, IL-17, TGFβ, and Immunoglobulin E (IgE) by enzyme-linked immunosorbent assay (ELISA).

The concentrations of INF-γ, IL-4, IL-17, TGFβ, and IgE in BALF were determined using commercially available ELISA kits INF-γ, ELISA Kit (LS-F7108), LifeSpan BioSciences, Inc USA; IL-4, ELISA kit, (DEIA208), Creative Diagnostics, USA; IL-17 ELISA Kit (E0115Ra), Bioassay Technology Laboratory, China; TGFβ ELISA Kit (670. 070. 128), Cell Sciences, Inc USA, and IgE ELISA Kit (E-EL-R0517) Elabsciences, USA according to the manufacturer's instructions.

- Measurement of Beclin-1 and P-62 by ELISA:

The concentrations of Beclin-1 and P-62 in the tissue lysate were determined using commercially available ELISA kits (Beclin-1, ELISA Kit (EK731452), AFG BioSciences, Inc USA; P-62, ELISA kit, (SL1363Ra), SunLong Biotech Co., LTD, China).

2.5.6. Immunohistochemistry (IHC) of Caspase 3

On adhesive slides, 5 μm tissue sections were cut and rehydrated. Heat-induced epitope retrieval step was performed, followed by peroxidase blocking. Rabbit Anti Caspase 3 Antibody, Polyclonal Antibody (LSBio (LifeSpan) Cat# LS-B3404-50, RRID: AB_10627102, Dil.: 10 μg/ml) was used in this IHC examination and it was carried out on paraffin sections and mounted on positively charged slides by using avidin–biotin-peroxidase complex (ABC) method. Sections from each group were incubated with the previously mentioned antibodies, then the reagents required for ABC method (Vectastain ABC-HRP kit, Vector laboratories) were added. Marker expression was labeled with peroxidase and colored with diaminobenzidine (DAB, produced by Sigma) to detect antigen–antibody complex. Negative controls were included using non-immune serum in place of the primary or secondary antibodies. IHC stained sections were examined using Leica microscope (CH9435 Hee56rbrugg) (Leica Microsystems, Switzerland).

2.5.7. Histopathology

Lung tissues of tested rats were sliced to 3–4 mm thick, fixed in 10 % neutral buffered formalin (10 % NBF), dehydrated in graded concentrations of ethanol, cleared in xylene, and embedded in paraffin. The paraffin blocks were sectioned with a microtome at (4—6 μm) thickness and dyed with Hematoxylin and Eosin (H&E) stain to study general tissue structure. H&E-stained sections were examined using Leica microscope (CH9435 Hee56rbrugg) (Leica Microsystems, Switzerland) (Bancroft and Gamble, 2008).
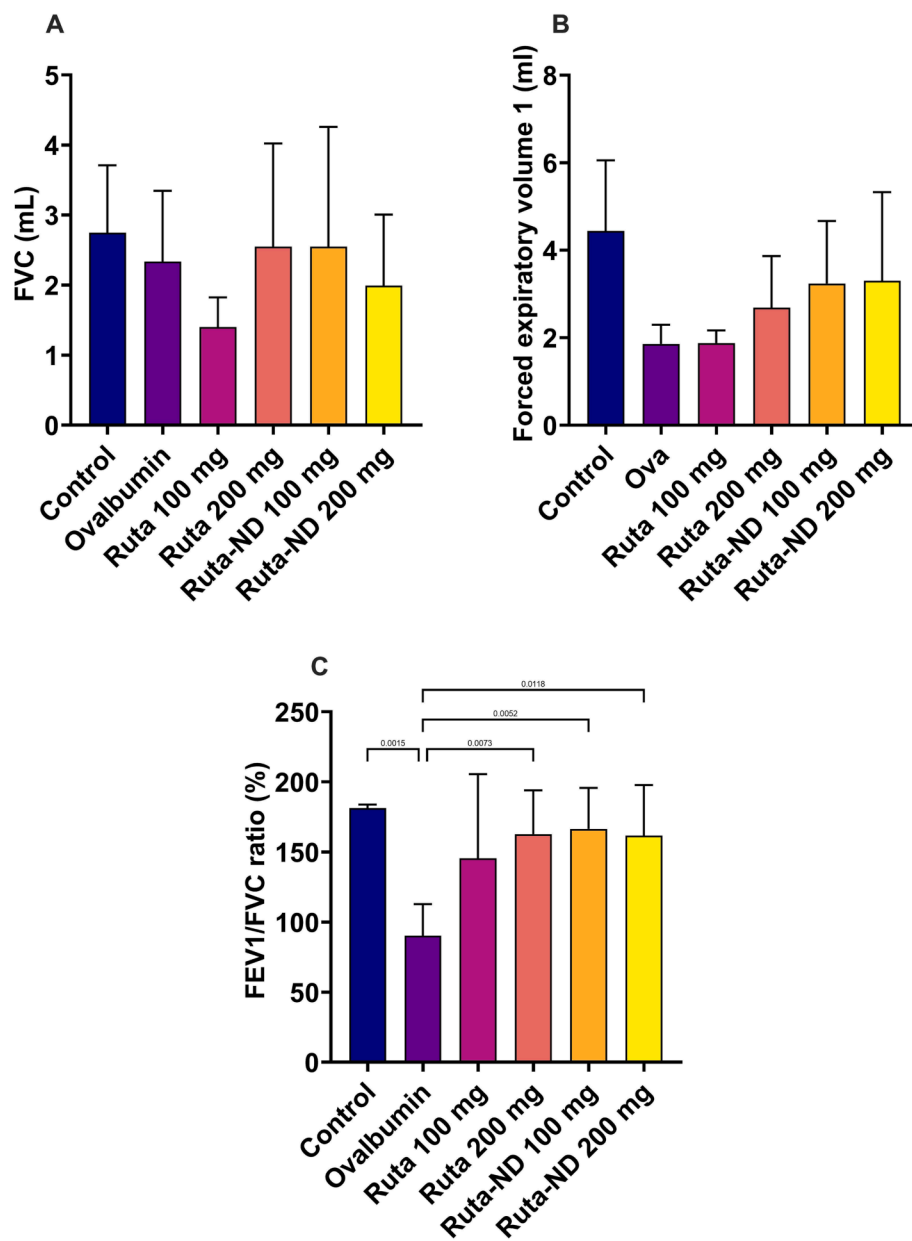
Fig. 5. A quantitative analysis of lung function tests shows (A) vital capacity, (B) forced expiratory volume 1 (FEV1), and (C) FEV1/FVC ratio. Data represented as mean $\pm$ SD.

2.6. UPLC-ESI-MS/MS analysis of total MeOH extract of R. Graveolens

UPLC-ESI-MS/MS analysis was performed using LC-MS/MS system (Nexera with LCMS-8045, Shimadzu Corporation, Kyoto, Japan)- HPLC (Nexera LC-30AD) equipped with an autosampler (SIL-30AC), temperature-controlled column oven (CTO-20AC) and photodiode array detector (LC-2030/2040) with detection wavelengths of 254 and with λ_{max} absorption at 220–400 nm and coupled to triple quadrupole mass spectrometer (Nexera with LCMS-8045, Shimadzu Corporation, Kyoto, Japan). LC-PDA-MS was equipped with RP-C18 UPLC column (shimpack 2 mm $\times$ 150 mm) possessing 2.7 μm particle size using acetonitrile (ACN)/0. 1 % HCOOH in H_2O in the following gradients [10 % ACN (0–2 min), 30 % CAN (2–5 min), 50 % ACN (5–15 min, 70 % ACN (15–25 min), 80 % ACN (25–28 min), 80 % ACN (28–30), 10 % ACN (30–33 min), with 0.2 ml/min flow rate. The positive mode was operated during LC-MS/MS with electrospray ionization (ESI). LC-MS/MS data were collected and processed by Lab Solutions software (Shimadzu, Kyoto, Japan).

2.6.1. Statistical analysis

GraphPad 9 version 9.4.1 was used in all the statistical analysis. Multiple comparisons using one-way ANOVA and Bonferroni as post hoc test. Results are illustrated as mean $\pm$ standard deviation (SD). For in-vivo study, sample size calculation was performed using open-source G* Power version 3.1.9.4, and with estimated power 80 % and α 0.05. Significance was indicated when $p \leq 0.05$.

3. Results

3.1. In vitro growth inhibition assay

The cytotoxicity of *R. graveolens* total MeOH extract (TE) and EtOAc, MeOH, and but. fractions were measured on BEAS-2B cells via MTT assay (Fig. 1). The tested samples showed inhibition of cell proliferation in a dose-dependent way. BEAS-2B cells were most sensitive to MeOH fraction with IC$_{50}$ of 111.24 $\pm$ 6.22 μg/ml followed by EtOAc fraction, TE, and but. fraction with IC$_{50}$ of 231.67 $\pm$ 13 μg/ml, 372.12 $\pm$ 20.8 μg/
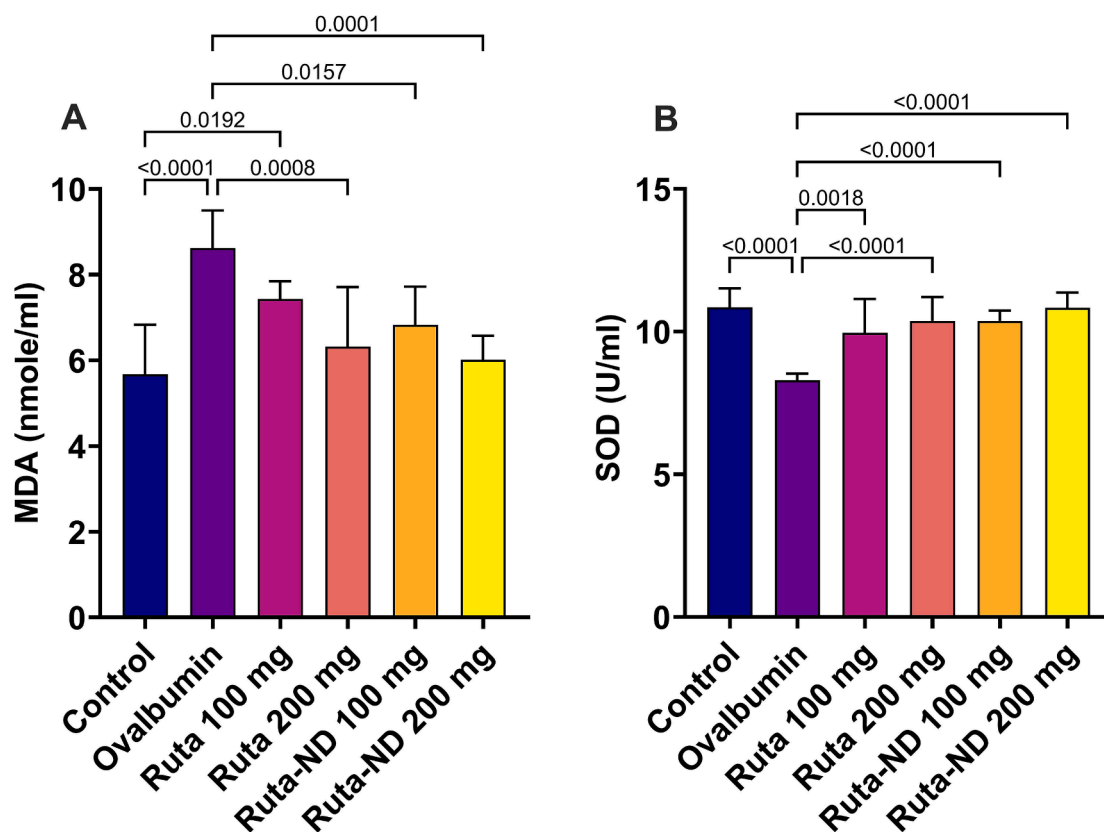
Fig. 6. A quantitative analysis of (A) MDA and (B) SOD in the bronchioalveolar lavage (BALF). Data represented as mean $\pm$ SD.

ml, 489.36 $\pm$ 27.4 µg/ml, respectively.

3.2. Gene expression of IL-17, TGF-β, IL-4 and IFN-γ, by q-PCR

The mRNA expression of IL-17, TGF-β, IL-4 were upregulated, while IFN-γ was downregulated in BEAS-2B cells treated with LPS. Pretreatment of BEAS-2B cells with IC_{50} and ½ IC_{50} of the TE and different fractions of *R. graveolens* significantly attenuated the LPS effect on the expression levels of IL-17, TGF-β, IL-4, and IFN-γ compared to the positive control group at $P < 0.0001$ (Fig. 2). IC_{50} of *R. graveolens* TE significantly decreased the expression of IL-17 to 0.272 $\pm$ 0.021, TGF-β to 0.348 $\pm$ 0.015, IL-4 to 0.267 $\pm$ 0.011, and increased considerably IFN-γ to 7.943 $\pm$ 0.25 when compared to other *R. graveolens* fractions at $P < 0.0001$. Accordingly, the TE was further examined by an *in-vivo* study to clarify its anti-asthmatic property.

3.3. UPLC-ESI-MS/MS characterization of total MeOH extract of R. Graveolens L

Altogether 58 secondary metabolites were tentatively identified in the total MeOH extract of *R. graveolens* using UPLC-ESI-MS/MS in positive ionization modes (Fig. 3). The identification of the compounds based on their MS, MS-MS fragmentation patterns, and the comparison with the data in the literature. The identified metabolites, which belong to different classes of metabolites (alkaloids, flavonoids, coumarins, phenolic acids), are summarized in Table 1 and ordered according to their retention time (Rt).

3.4. Characterization of Ruta-ND

In the current study, Ruta-ND was successfully prepared using a hot emulsification technique, with a loading efficiency of 47.37 % (the amount of extract in nanocubosomes relative to the total amounts

nanocubosomes' components). Results showed that the prepared system displayed a small PS (313.82 $\pm$ 33.10 nm) and a good size distribution since it has a PDI value of less than 0.5 (the mean PDI value was 0.39 $\pm$ 0.10). Also, the ZP of the prepared ND was found to be 31.20 $\pm$ 0.10 mV (Fig. 4 **B**). In addition, TEM of the nano-cubosomal system demonstrated non-aggregated polyangular nanoparticles of average size which is similar with the particle sizes data obtained by Zetasizer (Fig. 4 **C**).

3.5. In-vivo evaluation of the anti-asthmatic activity of Ruta-ND

3.5.1. Behavioral scoring
Table 2 revealed that Ova group exhibited a significant increment in the total scores of itching, sneezing, and runny nose compared to control rats. Treatment with Ruta extracts and Ruta-ND at different doses (100 and 200 mg/kg) decreased the overall score of these symptoms compared to the Ova group. However, no substantial difference existed between the treated groups and control rat.

3.5.2. Respiratory function measurements
Lung functions were recorded at the end of the experiment on the euthanizing day. No statistically significant difference was recorded between the groups regarding FVC and FEV1 shown in Fig. 5A,B. Regarding the FEV1/FVC ratio, there was a statistically marked decrease in the Ova group compared with the control (p = 0.015). While there was a significant statistical increase between the Ruta 200 mg and both doses of Ruta-ND treated groups compared to the Ova group (p = 0.0073, 0.0052, and 0.0118, respectively) as shown in Fig. 5**C.**

3.5.3. Oxidative stress biomarkers levels
Ruta extracts and Ruta-ND treated rats at the two doses displayed a significant reduction in the oxidative stress parameters compared to Ova-sensitized rat. Regarding MDA, there was a statistically significant reduction in the production of MDA in all of the treated groups, except
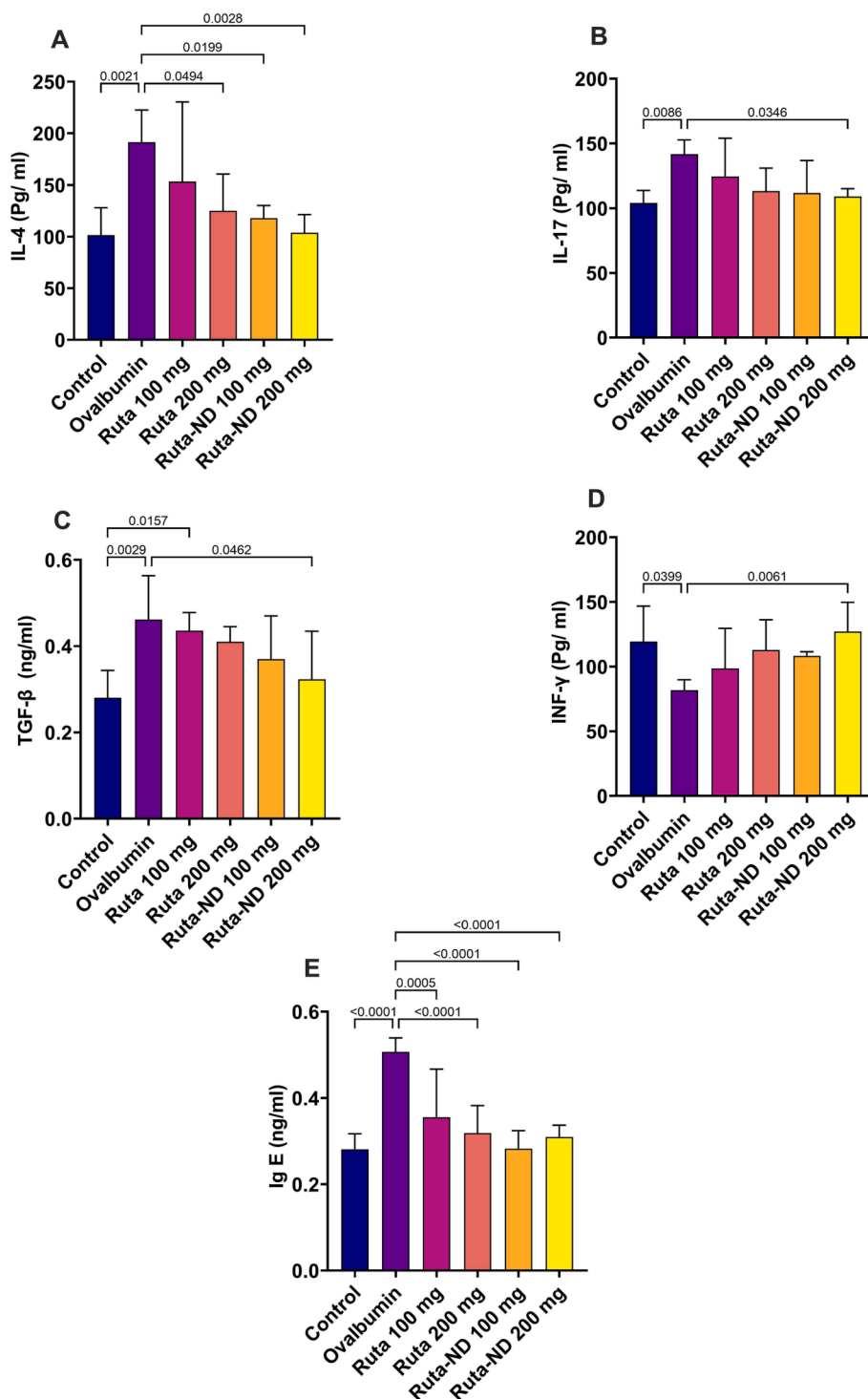
Fig. 7. A quantitative analysis of (A) IL-4, (B) IL-17, (C) TGFβ, (D) INF-γ, and (E) IgE in the BALF. Data represented as mean ± SD.

for Ruta exract at 100 mg/kg, compared to the Ova group, as shown in Fig. 6**A**. Moreover, SOD levels were restored to normal values in all treated groups. There was a statistically significant increase in the SOD levels in the treated groups compared to the Ova group, as shown in Fig. 6**B**.

3.5.4. INF-γ, IL-4, IL-17, TGFβ, and IgE levels in BALF

The BALF of the Ruta total MeOH extract 200 mg and both doses of Ruta-ND displayed a statistically significant reduction in IL-4 expression compared to the Ova group, as shown in Fig. 7**A**. While only Ruta-ND 200 mg showed a statistically significant reduction in IL-17 and TGF-β expression compared to Ova group (Fig. 7**B,C**). The expression of the INF-γ significantly increased in the BALF of Ruta-ND 200 mg compared to the Ova group, as shown in Fig. 7**D**. All the treated groups restored the normal levels of Ig-E production in the BALF. The Ova sensitiaed rats showed a statistically marked increment in the Ig-E production compared to all the Ruta-treated groups, as shown in Fig. 7**E**.

3.5.5. Beclin-1 and P-62 levels

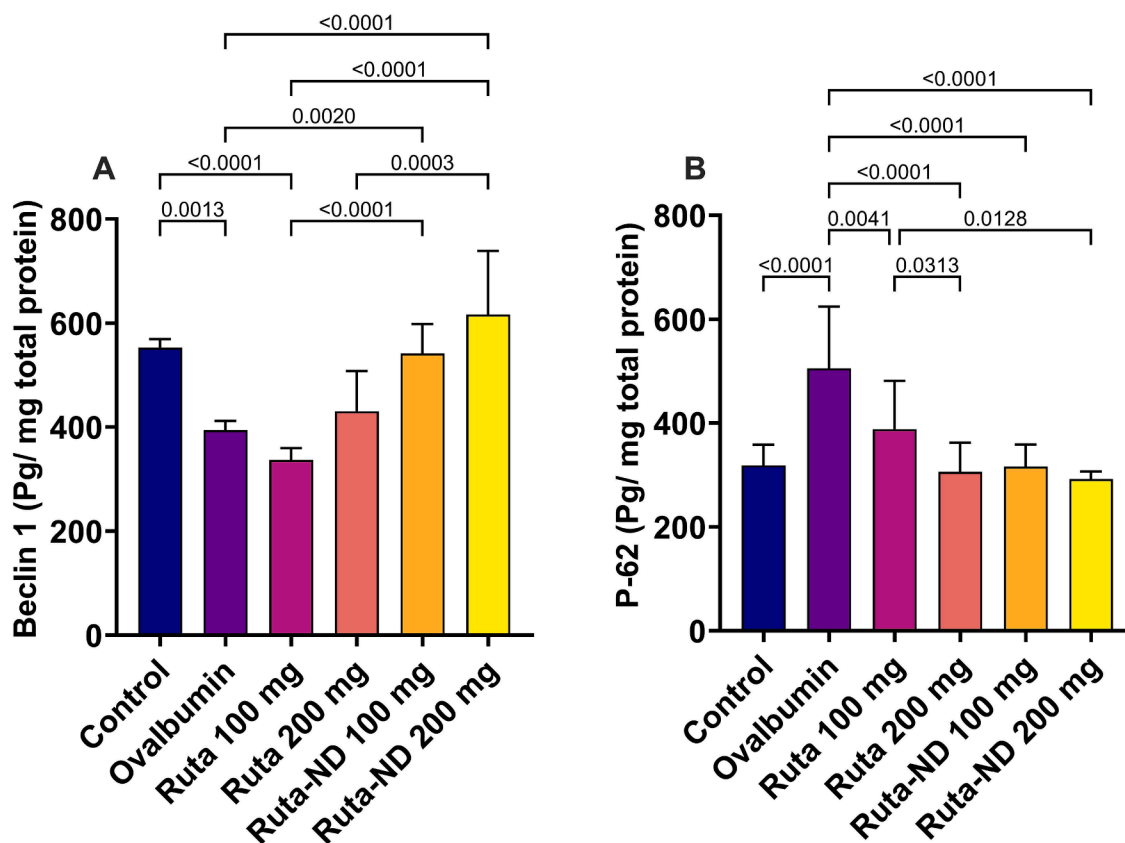Although the Ruta total MeOH extract group has no effect on Beclin-

Fig. 8. Autophagy parameters: a quantitative analysis of (A) Beclin-1 and (B) P-62 in the lung tissue. Data represented as mean $\pm$ SD.
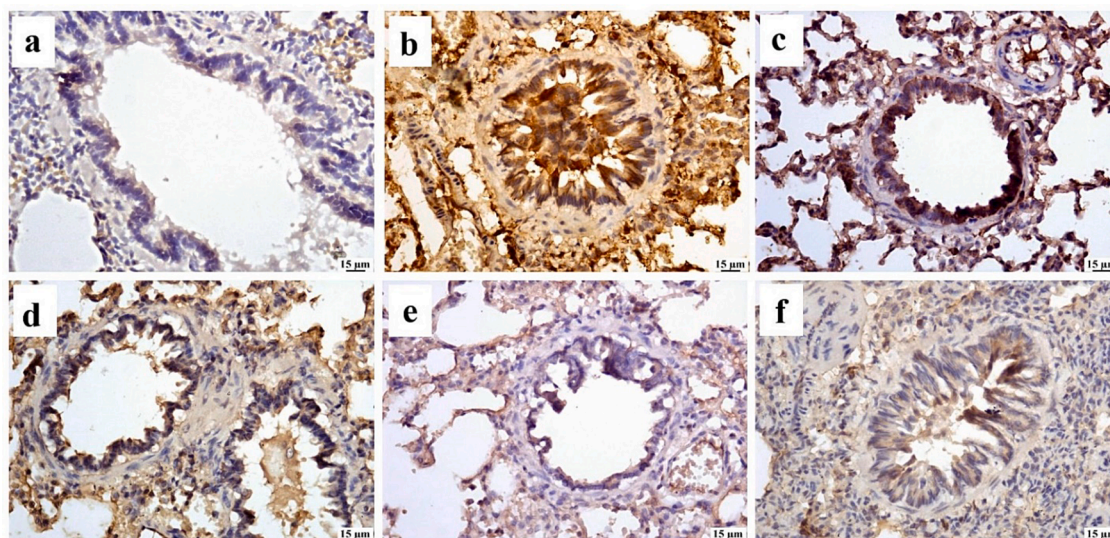

Fig. 9. Photomicrograph of lungs (Immune staining) showing limited mTOR expression in (a) control group, increased expression in (b) Ova group, moderate expression in both Ruta 100 mg (c) and Ruta 200 mg (d), marked reduction in mTOR expression in Ruta-ND 100 mg (e) and Ruta-ND 200 mg groups (f).

1 level in the lung tissue when compared to the Ova group. However, the levels of Beclin-1 in the Ruta-ND groups showed a statistically significant increase compared to Ova group as well as Ruta extract 100 mg. The Ova group displayed significantly lower Beclin-1 levels compared to the control group (Fig. 8A). There was a statistically significant reduction in the P-62 production in all the treated groups when compared to the Ova group. The Ova group showed a substantial increase in the P-62 levels compared to control rats (Fig. 8B).

3.5.6. mTOR and Caspase 3 expression

Lung tissue of the Ova group exhibited significant increase in mTOR expression in comparison to control group. All treated groups showed a substantial reduction in mTOR-positive staining. No significant difference was observed between Ruta total MeOH extract 100 mg and 200 mg groups. In comparison to the Ova group, Ruta-ND 100 mg and Ruta-ND 200 mg groups showed a significant decrease in mTOR expression in a dose-dependent manner (Figs. 9 and 10).

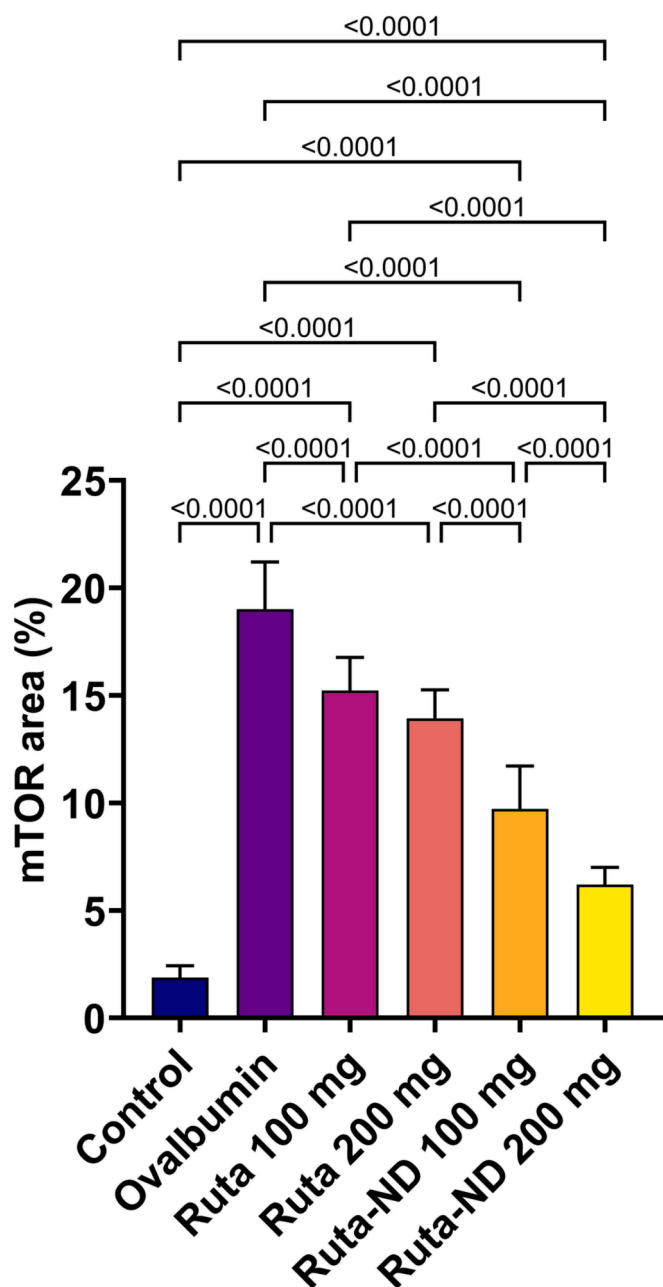Concerning caspase 3 expression, Lung tissue from the Ova Group

Fig. 10. Chart represents mTOR expression in lung tissue (area %) in different groups, data are presented as mean ± SEM. Significant difference was considered at P < 0.05.

highlighted the strongest Caspase 3 nuclear and cytoplasmic expression along collapsed alveoli and encircling bronchiole area, indicating enhanced apoptosis. All treated groups showed a reduction in Caspase 3 nuclear expression. It was noticed that the decrease of Caspase 3 nuclear expression was dose-dependent and that the Ruta-ND 200 mg showed the fewest Caspase 3 nuclear expression along the alveolar wall (Fig. 11).

3.5.7. Histopathological investigation

Histological examination showed that lung tissue from the Ova group was extensively damaged, as indicated by severe lung degeneration with collapsed alveoli, serious hemorrhage with infiltration of inflammatory cells in all tissue, and excessive hyperplasia in bronchioles epithelium (Fig. 12B). All treated groups showed recovery of deteriorating effects noticed in the Ova group. It was noticed that the recovery

percentage was increased by increasing the Ruta total MeOH extract doses and that the Ruta-ND 200 mg group showed normal existence of most alveoli with tiny amounts of hemorrhage, inflammatory cells, and accumulated fibers (Fig. 12C,D).

4. Discussion

There is a long history of using medicinal herbs to treat asthma in many different nations (Sugiura and I.M., 2008). In the present study, anti-inflammatory properties of the total extract (TE) and fractions (EtOAc, butanol, and MeOH) of *R. graveolens* herb were studied. Firstly, TE exhibited the most potential anti-inflammatory activity as manifested by significant decreased IL-17, TGF-β, IL-4, and significantly increased IFN-γ when compared to other *R. Graveolens* fractions. therefore, the metabolic contents, and therapeutic activity of TE in a rat model sensitized to OVA was studied.

The total MeOH extract as a potent anti-inflammatory agent was introduced into UPLC-ESI-MS/MS to explore its metabolites content. Characterization of the detected secondary metabolites afforded the identification of 58 compounds that belonging to several classes such as alkaloids (graveoline, graveolinine, skimmianine, kokusaginin, rutacridone, γ-Fagarine, dictamnine, etc.), flavonoids (rutin, vecenin-2, pinnarin, rutaretin, quercitrin, isoquercitrin, isorhamnetin 3-O-rutinoside, quercetin, etc….), coumarins (chalepin, chalepensin, psoralen, umbelliferone, scopoletin, xanthotoxin), and phenolic acids (caffeic acid, syringic acid, 5-caffeoylquinic acid, 4-caffeoylquinic acid).

NDs have been extensively utilized in drug delivery as they tend to improve the bioavailability of the administered drug and allow improved targeting in the body which consequently leads to enhancement in pharmacological efficacy and/or concomitant reduction in the required dose (Mudshinge et al., 2011). Accordingly, Ruta-ND with a small PS was prepared. Remarkably, small PS is important to improve cellular uptake, smaller-size nanoparticles (267.8 nm) exhibit two folds higher uptake efficiency than large-size ones (567.7 nm) (Um et al., 2003). The ZP was also measured for the prepared system to ensure its stability. It is documented that around ± 30 mv ZP values are required to ensure the stability of colloidal dispersions (Al-Mahallawi et al., 2021).

In the in vivo study, the *R. graveolens* TE ameliorated the alveolar damage, hemorrhage, and inflammatory cell infiltration caused by Ova sensitization. It was noted that *R. graveolens* therapeutic effect was dose-dependent. Moreover, both doses of Ruta-ND (100 and 200 mg/kg) were more effective than both doses of *Ruta* TE (100 and 200 mg/kg), which could be attributed to their small PS that enable a better uptake. To investigate the proposed lung protective mechanism of *R. graveolens*, we measured asthma behavioral score and lung function tests in the rat groups after the treatment as well as the levels of MDA, SOD, IFN-γ, IL-4, IL-17, and TGF-β, in BALF and Beclin-1, P-62 in lung tissue homogenate and caspase 3 expression in lung tissues, also all the groups were evaluated histopathologically by H&E.

The FEV1/FVC ratio is an important measure for the improvement of lung function in asthmatic patients (Wang et al., 2021). The treatment of asthmatic Wister rats with *R. graveolens* TE and both doses of Ruta-ND have corrected the FEV1/FVC ratio to the normal values in control rats. The improvement might be directly correlated with the antioxidant property of *R. graveolens*. These data agree with Mona et al., 2014 where antioxidant of rosiglitazone managed to improve FEV1/FVC ratio in guinea pigs' asthmatic model (El-Naa et al., 2014).

Oxidative stress may be involved in asthma pathogenesis (Omenaas et al., 2003; Stone and Yang, 2006). This oxidative stress observed in asthma patients could be caused by inflammation or is a causative factor in the pathogenesis of the disease. Reactive oxygen species (ROS) such as hydrogen peroxide (H_2O_2) transfer stimulating signals as a critical intracellular second messenger, resulting in the modulation of immune responses (Grievink et al., 1998). In bronchial asthma, oxidative stress exacerbates airway inflammation by stimulating several
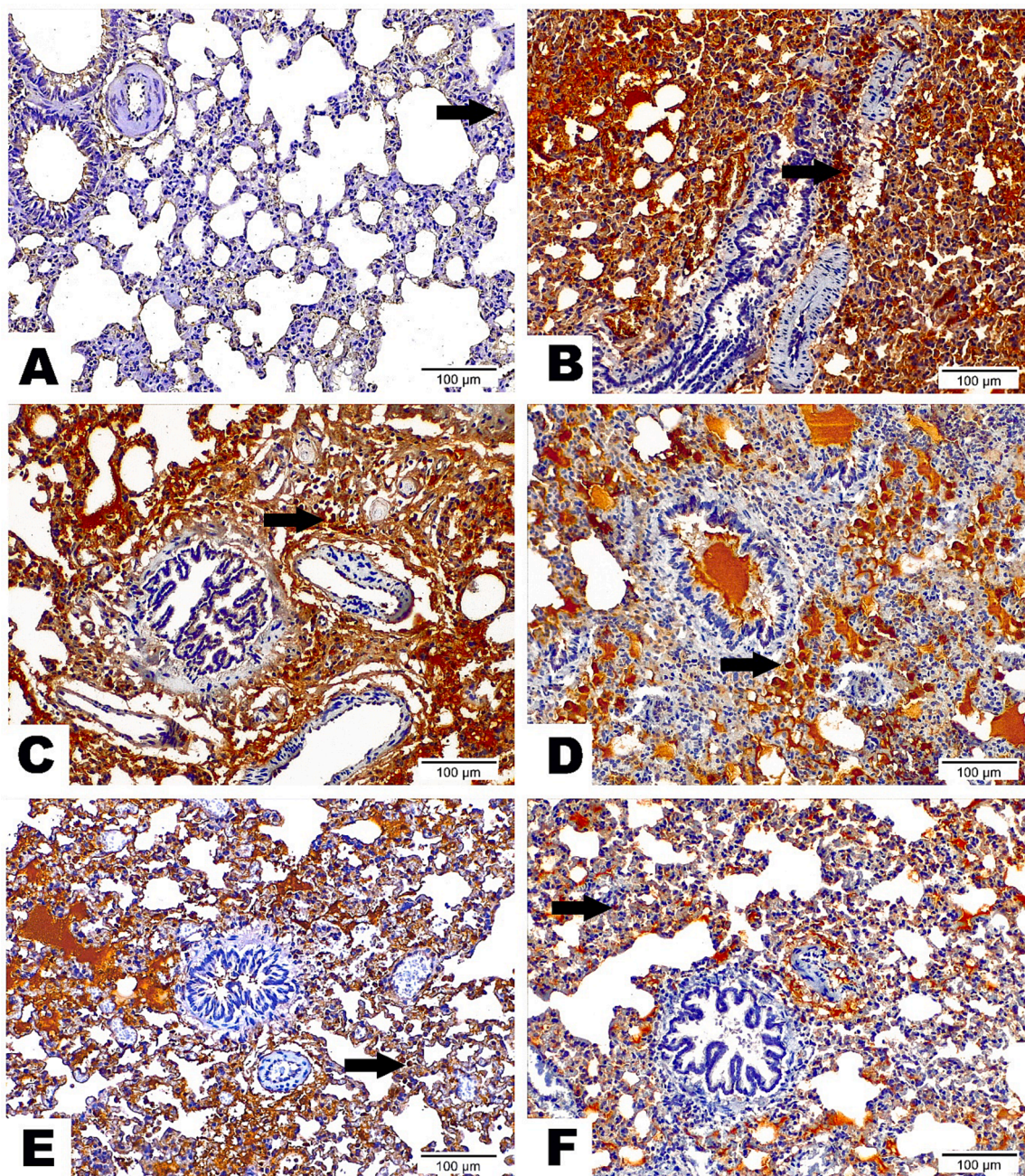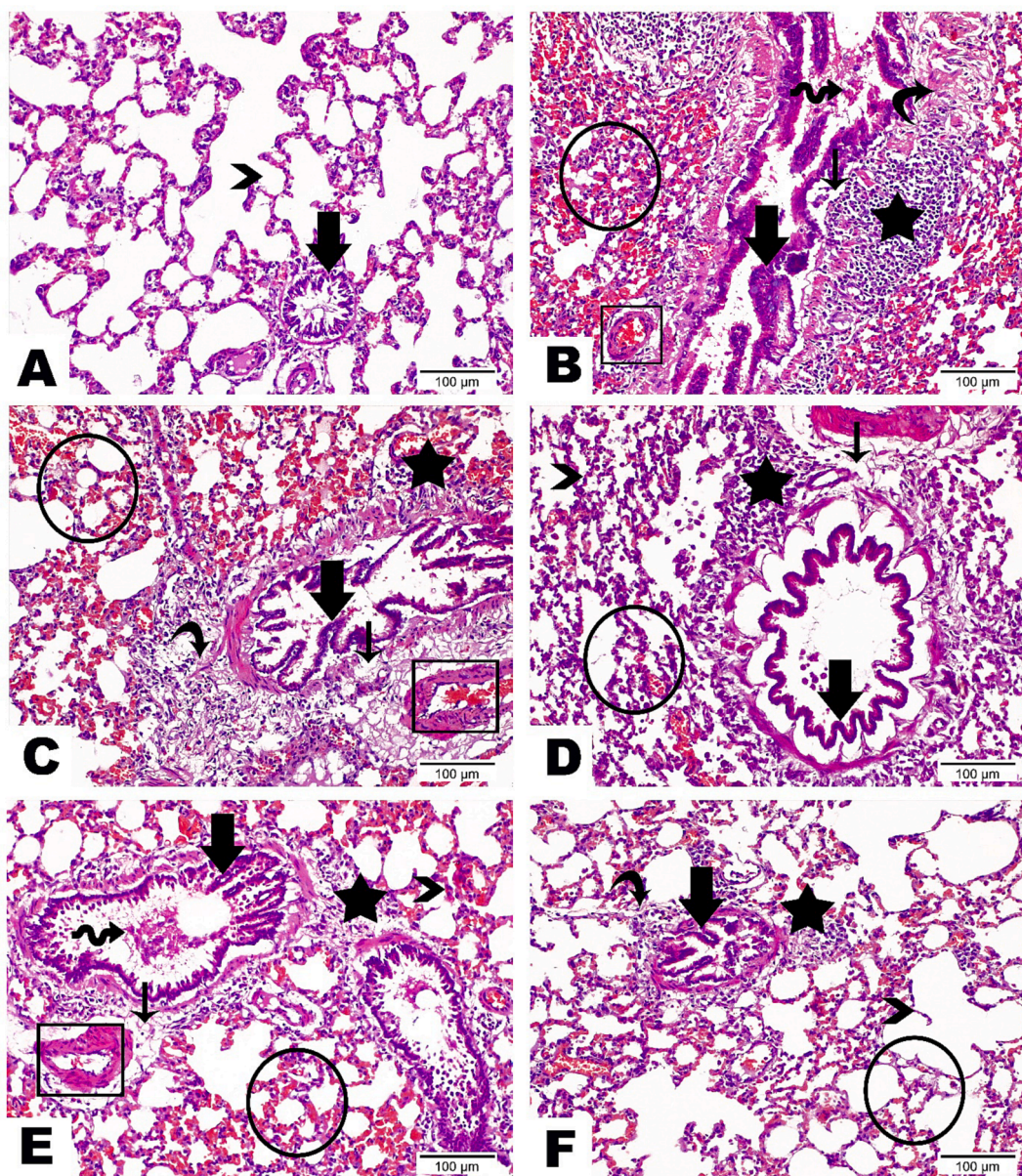
Fig. 11. Photomicrographs displayed the expression of Caspase 3 Antibody on lung sections among inspected groups as follows: (A) Lung Section from control group demonstrated scarce Caspase 3 nuclear reaction (arrow) along lung tissue. (B) Lung Section from Ova group highlighted the strongest Caspase 3 nuclear and cytoplasmic expression along collapsed alveoli as well as encircling bronchiole area (arrow). (C) Lung Section from Ruta 100 mg group underscored high Caspase 3 nuclear and cytoplasmic reaction (arrow) along alveolar wall and encircling bronchiole. (D) Lung Section from Ruta 200 mg group marked moderate Caspase 3 nuclear and cytoplasmic expression along collapsed alveoli and surrounded bronchiole (arrow). (E) Lung Section from Ruta-ND 100 mg group exposed moderate Caspase 3 nuclear expression (arrow) with a value beneath Ruta total MeOH extract 200 mg group. (F) Lung Section from Ruta-ND 200 mg group existed with a few Caspase 3 nuclear expression (arrow) along alveolar wall. (Caspase 3 Antibody, Magnification Power = x200 & Scale Bar = 100 μm).

proinflammatory mediators, increasing bronchial hyperresponsiveness, inducing bronchospasm, and increasing mucin production (Li and Nel, 2006; Terada, 2006; Motamed, 2014; Brown and Griendling, 2009; Elansary et al., 2020). Our results showed increased oxidative stress in Ova-sensitized rats as manifested by elevated MDA and reduced SOD levels in BALF. All *R. graveolens* treated groups showed a significant decrease in the MDA level compared to Ova-sensitized group except Ruta 100 mg, which showed a non-significant difference.

Regarding SOD level, all *R. graveolens* treated groups showed a significant increase in the SOD level compared to Ova-sensitized group. It was noted that there were no significant differences in MDA and SOD levels between Ruta 100 mg and 200 mg. These results indicate strong antioxidant properties of *R. graveolens* which was supported by previous studies (Asgharian et al., 2020; Pawankar et al., 2015). This strong antioxidant effect may be attributed to the high content of flavonoids, especially rutin and phenolic acids in *R. graveolens* (Park et al., 2009).

An important contributing element to the onset and progression of allergic airway inflammation, particularly allergic asthma, is inflammation (Kao et al., 2013). In this study, allergic airway inflammation was successfully demonstrated by a significant increase of inflammatory

Fig. 12. Photomicrographs presented the histopathological alterations along lung tissue sections of examined groups as follows: (A) Lung Section from control group displayed the standard assembly of alveoli (arrowhead) and bronchiole (thick arrow) inside lung tissue. (B) Lung Section from Ova group highlighted severe lung degeneration with collapsed alveoli and serious hemorrhage with infiltration of inflammatory cells in all tissue (circle). Bronchioles epithelium marked with desquamation (wave arrow), excessive hyperplasia in addition to its detachment from basement membrane (thick arrow). Subepithelial edema (thin arrow), aggregation of inflammatory cells (star), obvious increase in fibers amount (curve arrow), and congestion inside blood vessels (rectangle) were also detected. (C) Lung Section from Ruta 100 mg group emphasized deteriorating changes less than Ova group which demonstrated by little recovery of the collapsed alveoli, obvious decrease in serious hemorrhage as well as the number of inflammatory cells along alveolar wall (circle), partial decline in epithelial hyperplasia (thick arrow) and few amount of submucosal inflammatory cells (star). However clear expansion in edema (thin arrow) and fibers amount encircling bronchiole (curve arrow) were noticed in combination with congestion in blood vessels (rectangle). (D) Lung Section from Ruta 200 mg group disclosed moderate improvement that marked in thin irregular alveolar wall (arrowhead), few hemorrhage (circle), obvious normal bronchial epithelium (thick arrow), low number of aggregated inflammatory cells (star), in addition to edema leading to dispersion between fibers surrounding bronchiole (thin arrow). (E) Lung Section from Ruta-ND 100 mg group revealed high enhancement along alveolar wall architecture (arrowhead), excluding some hemorrhage dispersed throughout lung tissue (circle). Bronchial epithelium revealed desquamation (wave arrow) and some hyperplasia (thick arrow). Inflammatory cells (star) and fibers (thin arrow) are presented in a small amount. Observe the normal existence of blood vessels (rectangle). (F) Lung Section from Ruta-ND 200 mg group marked great development with normal existence of most alveoli (arrowhead). Hemorrhage (circle), inflammatory cells (star), and accumulated fibers (curve arrow) were recorded in tiny mounts. Bronchial epithelium recorded in its normal assembly (thick arrow). (Hematoxylin & Eosin staining, Magnification Power = x200 & Scale Bar = 100 μm).

mediators in the BALF of Ova-sensitized rats, such as IL-4, IL-17, TGF-β, and IgE, and a significant decrease of IFN-γ. Allergic inflammation was significantly inhibited by the treatment with Ruta-ND 100 mg and 200 mg. Levels of IFN-γ were increased dramatically in Ruta-ND 200 mg/kg than Ova-sensitized rats while all Ruta groups except Ruta 100 mg/kg managed to decrease IL-4 levels compared to Ova-sensitized rats. These

results come in agreement with Park and his colleagues, who reported that quercetin, main flavonoid of *R. graveolens*, managed to regulate Th1/Th2 balance as it reduced the levels of IL-4, a Th2 cytokine, and increased IFN-γ, a Th1 cytokine. This may be related to the ability of quercetin to suppress GATA-3, a transcription factor that promotes Th2 differentiation, and to increase Th1 transcription factor (T-bet)

expression in a mouse model of Ova-induced allergic airway inflammation (Park et al., 2009).

The results of our study also showed the ability of Ruta-ND 200 mg to reduce IL-17 and TGF-β levels than the Ova-sensitized group, significantly. These results are in harmony with different studies that were conducted to evaluate the effect of different natural products as an alternative therapy for asthma treatment (McCary, 2010; Lee et al., 2015; Liu et al., 2015; Abdala-Valencia et al., 2013).

The potent observed anti-inflammatory activity of R. graveolens TE may be related to the accumulated metabolites such as rutin and quercetin (Table 2), due to their anti-inflammatory and antioxidant properties as evident via suppressing lipid peroxidation and reducing oxidative stress in previous studies (Loonat and Amabeoku, 2014; Satari et al., 2021). Quercetin's anti-inflammatory activity may be due to its ability to prevent TNF-α-induced NF kappa (Salaritabar et al., 2017). Chung and his colleagues showed that kaempferol (Table 2) could considerably reduce the inflammatory process by reducing the inflammatory cells infiltration and the production of inflammatory cytokines and IgE antibodies in Ova induced airway inflammation in a mouse model of asthma (Chung et al., 2015). In addition, Mahat et al., showed that kaempferol's anti-inflammatory activity is mediated by the suppression of nitric oxide and nitric oxide-induced COX-2 enzyme activation, which further inhibits nitric oxide's cytotoxic effects and lowers the production of prostaglandin-E2 (Mahat and N.M.K., 2010).

It is yet unclear how autophagy contributes to allergic inflammatory reactions in the airways. Different experimental studies showed controversial results where; Gu and his colleagues showed that Ova-treated mice had decreased expression of autophagy-related genes such as Atg5, Lc3, and Beclin1 in lung homogenates and BALF macrophages accompanied by lower protein levels compared to control mice (Gu et al., 2017). Zhang and his colleagues showed raised expression of autophagy-related genes accompanied by higher protein levels in a mouse model of cockroach-allergen-induced allergic airway inflammation (Zhang et al., 2021). Our results demonstrated autophagy inhibition in Ova- sensitized group as manifested by decreased Beclin-1 levels and increased P62 levels in the lung homogenate. Ruta treatment restored autophagy as it significantly elevated Beclin-1 levels and reduced P62 levels.

Previous literature demonstrated a crosstalk between apoptosis and autophagy, including both positive and negative interactions (Ghavami et al., 2010; Zambrano and Yeh, 2016). In the present study, we demonstrated that Ova-sensitization inhibited autophagy as it decreased Beclin-1 levels and increased P62 Levels. Also, it induced apoptosis as manifested by increased Caspase 3 nuclear and cytoplasmic expression along collapsed alveoli as well as encircling bronchiole area in lung tissue. Beclin 1 network plays a central role in the cross-regulation between autophagy and apoptosis. Caspases-3 can cleave BECLIN1 at D124 and D149 yielding fragments lacking pro-autophagic capacity (Cho et al., 2009; Luo and Rubinsztein, 2010; Wirawan et al., 2010; Zhu et al., 2010). Additionally, it was shown that the C-terminal BECLIN1 fragment localizes to the mitochondria and is capable of releasing the pro-apoptotic proteins cytochrome *c* and HtrA2/Omi, suggesting the possibility of a positive feedback loop for apoptosis (Wirawan et al., 2010).

The increased apoptosis observed in Ova-sensitized group may be also linked to p62 accumulation which can promote the activation of caspase-8 mediating extrinsic apoptosis (Jin et al., 2009; Huang et al., 2013). Moreover, different dosage forms of *R. graveolens* managed to reverse these effects by restoring autophagy and inhibiting apoptosis.

5. Conclusion

In conclusion, the current study revealed that *R. graveolens* TE may be considered a potential treatment for allergic asthma. The TE as well as its ND of *R. graveolens* showed strong antioxidant and anti-inflammatory activities in the experimental allergic airway inflammation model, with a marked superiority of the ND system over the conventional extract. Antiasthmatic Effects of *R. graveolens* may also be attributed to autophagy induction and apoptosis inhibition. As an alternative to existing anti-allergic asthma medications, *R. graveolens*' abundance of antioxidants, anti-inflammatory, and antiallergic phytomolecules may prove beneficial in controlling allergy-induced asthma.

Appendix A. Supplementary material

Supplementary data to this article can be found online at https://doi.org/10.1016/j.jsps.2024.101968.

References

Abbas, A.K., Lichtman, A.H., Pillai, S., 2019. Basic Immunology: Functions and Disorders of the Immune System, 6e: Sae-E-Book. Elsevier India.

Abdala-Valencia, H., Berdnikovs, S., Cook-Mills, J.M., 2013. Vitamin E isoforms as modulators of lung inflammation. Nutrients 5, 4347–4363.

Albash, R., Yousry, C., Al-Mahallawi, A.M., Alaa-Eldin, A.A., 2021. Utilization of PEGylated cerosomes for effective topical delivery of fenticonazole nitrate: in-vitro characterization, statistical optimization, and in-vivo assessment. Drug Deliv. 28, 1–9. https://doi.org/10.1080/10717544.2020.1859000.

Al-Mahallawi, A.M., Abdelbary, A.A., El-Zahaby, S.A., 2021. Norfloxacin loaded nano-cubosomes for enhanced management of otitis externa: In vitro and in vivo evaluation. Int. J. Pharm. 600, 120490.

Asgharian, S., Hojjati, M.R., Ahrari, M., Bijad, E., Deris, F., Lorigooini, Z., 2020. Ruta graveolens and rutin, as its major compound: investigating their effect on spatial memory and passive avoidance memory in rats. Pharm. Biol. 58, 447–453. https://doi.org/10.1080/13880209.2020.1762669.

Bancroft, J.D., Gamble, M., 2008. Theory and practice of histology techniques. Churchill Livingstone Elsevier Lond. P83–P.

Bei, D., Marszalek, J., Youan, B.-B.-C., 2009. Formulation of Dacarbazine-loaded Cubosomes—Part II: Influence of Process Parameters. AAPS PharmSciTech 10, 1040–1047. https://doi.org/10.1208/s12249-009-9296-0.

Biavatti, M.W., 2007. Ethnopharmacognostic survey on botanical compendia for potential cosmeceutic species from Atlantic Forest.

Brown, D.I., Griendling, K.K., 2009. Nox proteins in signal transduction. Free Radic. Biol. Med. 47, 1239–1253. https://doi.org/10.1016/j.freeradbiomed.2009.07.023.

Cho, D.-H., Jo, Y.K., Hwang, J.J., Lee, Y.M., Roh, S.A., Kim, J.C., 2009. Caspase-mediated cleavage of ATG6/Beclin-1 links apoptosis to autophagy in HeLa cells. Cancer Lett. 274, 95–100. https://doi.org/10.1016/j.canlet.2008.09.004.

Chung, M.J., Pandey, R.P., Choi, J.W., Sohng, J.K., Choi, D.J., Park, Y.I., 2015. Inhibitory effects of kaempferol-3-O-rhamnoside on ovalbumin-induced lung inflammation in a mouse model of allergic asthma. Int. Immunopharmacol. 25, 302–310. https://doi.org/10.1016/j.intimp.2015.01.031.

Colucci-D'Amato, L., Cimaglia, G., 2020. Ruta graveolens as a potential source of neuroactive compounds to promote and restore neural functions. J. Tradit. Complement. Med. Nutraceuticals Diet Regimens Human Health Dis. 10, 309–314. https://doi.org/10.1016/j.jtcme.2020.05.002.

Cryns, V., Yuan, J., 1998. Proteases to die for. Genes Dev. 12, 1551–1570. https://doi.org/10.1101/gad.12.11.1551.

Dharmage, S.C., Perret, J.L., Custovic, A., 2019. Epidemiology of Asthma in Children and Adults. Front. Pediatr. 7, 246. https://doi.org/10.3389/fped.2019.00246.

Duncan, C., 2003. Reduced eosinophil apoptosis in induced sputum correlates with asthma severity. Eur. Respir. J. 22, 484–490.

El Said, H.S., Lalatsa, A., Al-Mahallawi, A.M., Saddar El Leithy, E., Ghorab, D.M., 2022. Vilazodone-phospholipid mixed micelles for enhancing oral bioavailability and reducing pharmacokinetic variability between fed and fasted states. Int. J. Pharm. 625, 122080 https://doi.org/10.1016/j.ijpharm.2022.122080.

Elansary, H.O., Szopa, A., Kubica, P., Ekiert, H., El-Ansary, D.O., Al-Mana, A.F., Mahmoud, E.A., 2020. Polyphenol Content and Biological Activities of Ruta graveolens L. and Artemisia abrotanum L., Northern Saudi Arabia. Processes 8, 531. https://doi.org/10.3390/pr8050531.

El-Naa, M.M., El-Refaei, M.F., Nasif, W.A., El-Brairy, A.I., 2014. Emerging role of a peroxisome proliferator-activated receptor-gamma (PPAR-γ) agonist in bronchial asthma in vivo: antioxidant activity and the down-regulation of inflammatory factors. Biochem. Lett. 10, 1–13. https://doi.org/10.21608/blj.2014.63402.

Enari, M., Sakahira, H., Yokoyama, H., Okawa, K., Iwamatsu, A., Nagata, S., 1998. A caspase-activated DNase that degrades DNA during apoptosis, and its inhibitor ICAD. Nature 391, 43–50. https://doi.org/10.1038/34112.

Fahmy, A.M., Hassan, M., El-Setouhy, D.A., Tayel, S.A., Al-Mahallawi, A.M., 2021. Statistical optimization of hyaluronic acid enriched ultradeformable elastosomes for ocular delivery of voriconazole via Box-Behnken design: in vitro characterization

and in vivo evaluation. Drug Deliv. 28, 77–86. https://doi.org/10.1080/10717544.2020.1858997.

Farag, D.B.E., Yousry, C., Al-Mahallawi, A.M., El-Askary, H.I., Meselhy, M.R., AbuBakr, N., 2022. The efficacy of Origanum majorana nanocubosomal systems in ameliorating submandibular salivary gland alterations in streptozotocin-induced diabetic rats. Drug Deliv. 29, 62–74. https://doi.org/10.1080/10717544.2021.2018522.

Gera, M., Sharma, N., Ghosh, M., Huynh, D.L., Lee, S.J., Min, T., Kwon, T., Jeong, D.K., 2017. Nanoformulations of curcumin: an emerging paradigm for improved remedial application. Oncotarget 8, 66680. https://doi.org/10.18632/oncotarget.19164.

Ghavami, S., E.M., A., SR, Chazin, W.J., Klonisch, T., Halayko, A.J., McNeill, K.D., Hashemi, M., Kerkhoff, C., Los, M., 2010. S100A8/A9 induces autophagy and apoptosis via ROS-mediated cross-talk between mitochondria and lysosomes that involves BNIP3. Cell Res. 20, 314–31.

Grievink, L., Smit, H.A., Ocké, M.C., van 't Veer, P., Kromhout, D., 1998. Dietary intake of antioxidant (pro)-vitamins, respiratory symptoms and pulmonary function: the MORGEN study. Thorax 53, 166–171. https://doi.org/10.1136/thx.53.3.166.

Gu, W., Cui, R., Ding, T., Li, X., Peng, J., Xu, W., Han, F., Guo, X., 2017. Simvastatin alleviates airway inflammation and remodelling through up-regulation of autophagy in mouse models of asthma. Respirol. Carlton Vic 22, 533–541. https://doi.org/10.1111/resp.12926.

Han, Y.H., Park, W.H., 2009. Growth inhibition in antimycin A treated-lung cancer Calu-6 cells via inducing a G1 phase arrest and apoptosis. Lung Cancer Amst. Neth. 65, 150–160. https://doi.org/10.1016/j.lungcan.2008.11.005.

Harat, Z.N., Sadeghi, M.R., Sadeghipour, H.R., Kamalinejad, M., Eshraghian, M.R., 2008. Immobilization effect of Ruta graveolens L. on human sperm: a new hope for male contraception. J. Ethnopharmacol. 115, 36–41. https://doi.org/10.1016/j.jep.2007.09.004.

Hasnain, S.M., 2016. Emerging status of asthma, allergic rhinitis and eczema in the Middle East. Glob. Health 7, 128–136.

Hou, X., Wan, H., Ai, X., Shi, Y., Ni, Y., Tang, W., Shi, G., 2016. Histone deacetylase inhibitor regulates the balance of Th17/Treg in allergic asthma. Clin. Respir. J. 10, 371–379. https://doi.org/10.1111/crj.12227.

Huang, S., Okamoto, K., Yu, C., Sinicrope, F.A., 2013. p62/sequestosome-1 up-regulation promotes ABT-263-induced caspase-8 aggregation/activation on the autophagosome. J. Biol. Chem. 288, 33654–33666. https://doi.org/10.1074/jbc.M113.518134.

Huntley, A., Ernst, E., 2000. Herbal medicines for asthma: a systematic review. Thorax 55, 925–929. https://doi.org/10.1136/thorax.55.11.925.

Jang, T.Y., Park, C.-S., Kim, K.-S., Heo, M.-J., Kim, Y.H., 2014. Benzaldehyde suppresses murine allergic asthma and rhinitis. Int. Immunopharmacol. 22, 444–450. https://doi.org/10.1016/j.intimp.2014.07.029.

Jiang, X., Fang, L., Wu, H., Mei, X., He, F., Ding, P., Liu, R., 2017. TLR2 Regulates Allergic Airway Inflammation and Autophagy Through PI3K/Akt Signaling Pathway. Inflammation 40, 1382–1392. https://doi.org/10.1007/s10753-017-0581-x.

Jin, Z., Li, Y., Pitti, R., Lawrence, D., Pham, V.C., Lill, J.R., Ashkenazi, A., 2009. Cullin3-based polyubiquitination and p62-dependent aggregation of caspase-8 mediate extrinsic apoptosis signaling. Cell 137, 721–735. https://doi.org/10.1016/j.cell.2009.03.015.

Kao, H.-F., Chang-Chien, P.-W., Chang, W.-T., Yeh, T.-M., Wang, J.-Y., 2013. Propolis inhibits TGF-β1-induced epithelial-mesenchymal transition in human alveolar epithelial cells via PPARγ activation. Int. Immunopharmacol. 15, 565–574. https://doi.org/10.1016/j.intimp.2012.12.018.

Kim, Y.-H., Choi, Y.-J., Lee, E.-J., Kang, M.-K., Park, S.-H., Kim, D.Y., Oh, H., Park, S.-J., Kang, Y.-H., 2017. Novel glutathione-containing dry-yeast extracts inhibit eosinophilia and mucus overproduction in a murine model of asthma. Nutr. Res. Pract. 11, 461–469. https://doi.org/10.4162/nrp.2017.11.6.461.

Lee, K.-P., Kang, S., Park, S.-J., Kim, J.-M., Lee, J.-M., Lee, A.-Y., Chung, H.-Y., Choi, Y.-W., Lee, Y.-G., Im, D.-S., 2015. Anti-allergic effect of α-cubebenoate isolated from Schisandra chinensis using in vivo and in vitro experiments. J. Ethnopharmacol. 173, 361–369. https://doi.org/10.1016/j.jep.2015.07.049.

Li, N., Nel, A.E., 2006. Role of the Nrf2-mediated signaling pathway as a negative regulator of inflammation: implications for the impact of particulate pollutants on asthma. Antioxid. Redox Signal. 8, 88–98.

Liang, X.H., Kleeman, L.K., Jiang, H.H., Gordon, G., Goldman, J.E., Berry, G., Herman, B., Levine, B., 1998. Protection against Fatal Sindbis Virus Encephalitis by Beclin, a Novel Bcl-2-Interacting Protein. J. Virol. 72, 8586–8596. https://doi.org/10.1128/jvi.72.11.8586-8596.1998.

Liang, X.H., Jackson, S., Seaman, M., Brown, K., Kempkes, B., Hibshoosh, H., Levine, B., 1999. Induction of autophagy and inhibition of tumorigenesis by beclin 1. Nature 402, 672–676. https://doi.org/10.1038/45257.

Liu, Y.-N., Zha, W.-J., Ma, Y., Chen, F.-F., Zhu, W., Ge, A., Zeng, X.-N., Huang, M., 2015. Galangin attenuates airway remodelling by inhibiting TGF-β1-mediated ROS generation and MAPK/Akt phosphorylation in asthma. Sci. Rep. 5, 11758. https://doi.org/10.1038/srep11758.

Loonat, F., Amabeoku, G.J., 2014. Antinociceptive, anti-inflammatory and antipyretic activities of the leaf methanol extract of Ruta graveolens L. (Rutaceae) in mice and rats. Afr. J. Tradit. Complement. Altern. Med. 11, 173–181.

Luo, S., Rubinsztein, D.C., 2010. Apoptosis blocks Beclin 1-dependent autophagosome synthesis: an effect rescued by Bcl-xL. Cell Death Differ. 17, 268–277. https://doi.org/10.1038/cdd.2009.121.

Ma, C., Ma, Z., Fu, Q., Ma, S., 2014. Anti-asthmatic effects of baicalin in a mouse model of allergic asthma. Phytother. Res. PTR 28, 231–237. https://doi.org/10.1002/ptr.4983.

Mahat, M.Y., N.M.K., S.L.V., 2010. Modulation of the cyclooxygenase pathway via inhibition of nitric oxide production contributes to the anti-inflammatory activity of kaempferol. Eur. J. Pharmacol. 642, 169–176.

McCary, J.-M.-C.-M., 2010. Isoforms of vitamin E differentially regulate inflammation. Endocr. Metab. Immune Disord.-Drug Targets 10, 348–366.

Meepagala, K.M., Schrader, K.K., Wedge, D.E., Duke, S.O., 2005. Algicidal and antifungal compounds from the roots of Ruta graveolens and synthesis of their analogs. Phytochemistry 66, 2689–2695. https://doi.org/10.1016/j.phytochem.2005.09.019.

Miguel, E.S., Rue, 2003. (Rutaceae) in traditional Spain: frequency and distribution of its medicinal and symbolic applications. Econ. Bot. 57, 231–244.

Motamed, S.M., 2014. Evaluation of antioxidant activity of Ruta graveolens L. extract on inhibition of lipid peroxidation and DPPH radicals and the effects of some external factors on plant extract's potency. Res. J. Pharmacogn. 1, 45–50.

Mudshinge, S.R., Deore, A.B., Patil, S., Bhalgat, C.M., 2011. Nanoparticles: Emerging carriers for drug delivery. Saudi Pharm. J. SPJ 19, 129–141. https://doi.org/10.1016/j.jsps.2011.04.001.

Mukherjee, A.B., Zhang, Z., 2011. Allergic asthma: influence of genetic and environmental factors. J. Biol. Chem. 286, 32883–32889. https://doi.org/10.1074/jbc.R110.197046.

Nadeem, A., 2015. Proteinase activated receptor-2-mediated dual oxidase-2 up-regulation is involved in enhanced airway reactivity and inflammation in a mouse model of allergic asthma. Immunology 145, 391–403.

Nelson, H.S., 2001. The importance of allergens in the development of asthma and the persistence of symptoms. Dis.–Mon DM 47, 5–15. https://doi.org/10.1067/mda.2000.da0470005.

Nylander, T., Mattisson, C., Razumas, V., Miezis, Y., Håkansson, B., 1996. A study of entrapped enzyme stability and substrate diffusion in a monoglyceride-based cubic liquid crystalline phase. Colloids Surf. Physicochem. Eng. Asp. 114, 311–320. https://doi.org/10.1016/0927-7757(96)03563-7.

Ojala, T., Remes, S., Haansuu, P., Vuorela, H., Hiltunen, R., Haahtela, K., Vuorela, P., 2000. Antimicrobial activity of some coumarin containing herbal plants growing in Finland. J. Ethnopharmacol. 73, 299–305. https://doi.org/10.1016/s0378-8741(00)00279-8.

Omenaas, E., Fluge, O., Buist, A.S., Vollmer, W.M., Gulsvik, A., 2003. Dietary vitamin C intake is inversely related to cough and wheeze in young smokers. Respir. Med. 97, 134–142. https://doi.org/10.1053/rmed.2003.1439.

Packard, K.A., Khan, M.M., 2003. Effects of histamine on Th1/Th2 cytokine balance. Int. Immunopharmacol. 3, 909–920. https://doi.org/10.1016/S1567-5769(02)00235-7.

Painter, J.D., Galle-Treger, L., Akbari, O., 2020. Role of Autophagy in Lung Inflammation. Front. Immunol. 11.

Papiris, S.A., Manali, E.D., Kolilekas, L., Triantafillidou, C., Tsangaris, I., 2009. Acute severe asthma: new approaches to assessment and treatment. Drugs 69, 2363–2391. https://doi.org/10.2165/11319930-000000000-00000.

Park, H., Lee, C.-M., Jung, I.D., Lee, J.S., Jeong, Y., Chang, J.H., Chun, S.-H., Kim, M.-J., Choi, I.-W., Ahn, S.-C., Shin, Y.K., Yeom, S.-R., Park, Y.-M., 2009. Quercetin regulates Th1/Th2 balance in a murine model of asthma. Int. Immunopharmacol. 9, 261–267. https://doi.org/10.1016/j.intimp.2008.10.021.

Pawankar, R., Hayashi, M., Yamanishi, S., Igarashi, T., 2015. The paradigm of cytokine networks in allergic airway inflammation. Curr. Opin. Allergy Clin. Immunol. 15, 41–48. https://doi.org/10.1097/ACI.0000000000000129.

Pollio, A., De Natale, A., Appetiti, E., Aliotta, G., Touwaide, A., 2008. Continuity and change in the Mediterranean medical tradition: Ruta spp. (rutaceae) in Hippocratic medicine and present practices. J. Ethnopharmacol. 116, 469–482. https://doi.org/10.1016/j.jep.2007.12.013.

Poole, J.A., 2014. Asthma is a major noncommunicable disease affecting over 230 million people worldwide and represents the most common chronic disease among children. Int. Immunopharmacol. 23, 315. https://doi.org/10.1016/j.intimp.2014.09.013.

Preethi, K., Kuttan, G., Kuttan, R., 2006. Anti-tumour activity of Ruta graveolens extract. Asian Pac. J. Cancer Prev. 7, 439.

Racanelli, A.C., 2018. Autophagy and inflammation in chronic respiratory disease. Autophagy 14, 221–232.

Raghav, S.K., Gupta, B., Shrivastava, A., Das, H.R., 2007. Inhibition of lipopolysaccharide-inducible nitric oxide synthase and IL-1β through suppression of NF-κB activation by 3-(1′-1′-dimethyl-allyl)-6-hydroxy-7-methoxy-coumarin isolated from Ruta graveolens L. Eur. J. Pharmacol. 560, 69–80. https://doi.org/10.1016/j.ejphar.2007.01.002.

Ratheesh, M., 2011. Inhibitory effect of Ruta graveolens L. on oxidative damage, inflammation and aortic pathology in hypercholesteromic rats. Exp. Toxicol. Pathol. 63, 285–290.

Ratheesh, M., Shyni, G.L., Helen, A., 2009. Methanolic extract of Ruta graveolens L. inhibits inflammation and oxidative stress in adjuvant induced model of arthritis in rats. Inflammopharmacology 17, 100–105. https://doi.org/10.1007/s10787-009-8044-0.

Sakat, M.S., Kilic, K., Kandemir, F.M., Yildirim, S., Sahin, A., Kucukler, S., Saglam, Y.S., 2018. The ameliorative effect of berberine and coenzyme Q10 in an ovalbumin-induced allergic rhinitis model. Eur. Arch. Otorhinolaryngol. 275, 2495–2505. https://doi.org/10.1007/s00405-018-5104-3.

Salaritabar, A., Darvishi, B., Hadjiakhoondi, F., Manayi, A., Sureda, A., Nabavi, S.F., Fitzpatrick, L.R., Nabavi, S.M., Bishayee, A., 2017. Therapeutic potential of flavonoids in inflammatory bowel disease: A comprehensive review. World J. Gastroenterol. 23, 5097–5114. https://doi.org/10.3748/wjg.v23.i28.5097.

Satari, A., Ghasemi, S., Habtemariam, S., Asgharian, S., Lorigooini, Z., 2021. Rutin: A Flavonoid as an Effective Sensitizer for Anticancer Therapy; Insights into Multifaceted Mechanisms and Applicability for Combination Therapy. Evid.-Based

Complement. Altern. Med. ECAM 2021, 9913179. https://doi.org/10.1155/2021/9913179.

Schnyder-Candrian, S., 2006. Interleukin-17 is a negative regulator of established allergic asthma. J. Exp. Med. 203, 2715–2725.

Spinozzi, F., de Benedictis, D., de Benedictis, F.M., 2008. Apoptosis, airway inflammation and anti-asthma therapy: from immunobiology to clinical application. Pediatr. Allergy Immunol. Off. Publ. Eur. Soc. Pediatr. Allergy Immunol. 19, 287–295. https://doi.org/10.1111/j.1399-3038.2007.00668.x.

Stone, J.R., Yang, 2006. Suping Hydrogen peroxide: a signaling messenger. Antioxid. Redox Signal. 8, 243–270.

Sugiura, H.I.M., 2008. Oxidative and nitrative stress in bronchial asthma. Antioxid. Redox Signal. 10, 785–797.

Tao, B., 2015. Imbalance of peripheral Th17 and regulatory T cells in children with allergic rhinitis and bronchial asthma. Iran. J. Allergy Asthma Immunol. 273–279.

Terada, L.S., 2006. Specificity in reactive oxidant signaling: think globally, act locally. J. Cell Biol. 174, 615–623. https://doi.org/10.1083/jcb.200605036.

Um, J.Y., Chung, H., Kim, K.S., Kwon, I.C., Jeong, S.Y., 2003. In vitro cellular interaction and absorption of dispersed cubic particles. Int. J. Pharm. 253, 71–80.

Vignola, A.M., 2000. Apoptosis and airway inflammation in asthma. Apoptosis 5, 473–485.

Wang, J., Li, X., Wang, C., Li, Y., Wang, J., Fang, R., Wang, J., Chen, J., Dong, J., 2021. Exposure to di-(2-ethylhexyl) phthalate reduces secretion of GDNF via interfering with estrogen pathway and downregulating ERK/c-fos signaling pathway in astrocytes. Food Chem. Toxicol. 158, 112592 https://doi.org/10.1016/j.fct.2021.112592.

Wirawan, E., Vande Walle, L., Kersse, K., Cornelis, S., Claerhout, S., Vanoverberghe, I., Roelandt, R., De Rycke, R., Verspurten, J., Declercq, W., Agostinis, P., Vanden Berghe, T., Lippens, S., Vandenabeele, P., 2010. Caspase-mediated cleavage of Beclin-1 inactivates Beclin-1-induced autophagy and enhances apoptosis by promoting the release of proapoptotic factors from mitochondria. Cell Death Dis. 1, e18–e. https://doi.org/10.1038/cddis.2009.16.

Yoshii, S.R., Mizushima, N., 2017. Monitoring and Measuring Autophagy. Int. J. Mol. Sci. 18, 1865. https://doi.org/10.3390/ijms18091865.

Yue, Z., Zhong, Y., 2010. From a Global View to Focused Examination: Understanding Cellular Function of Lipid Kinase VPS34-Beclin 1 Complex in Autophagy. J. Mol. Cell Biol. 2, 305–307. https://doi.org/10.1093/jmcb/mjq028.

Zambrano, J., Yeh, E.S., 2016. Autophagy and Apoptotic Crosstalk: Mechanism of Therapeutic Resistance in HER2-Positive Breast Cancer. Breast Cancer Basic Clin. Res. 10, 13–23. https://doi.org/10.4137/BCBCR.S32791.

Zeki, A., 2016. Autophagy in airway diseases: a new frontier in human asthma? Allergy 71, 5–14.

Zhang, Y., Do, D.C., Hu, X., Wang, J., Zhao, Y., Mishra, S., Zhang, X., Wan, M., Gao, P., 2021. CaMKII oxidation regulates cockroach allergen-induced mitophagy in asthma. J. Allergy Clin. Immunol. 147, 1464–1477.e11. https://doi.org/10.1016/j.jaci.2020.08.033.

Zhou, C., 2011. Epithelial apoptosis and loss in airways of children with asthma. J. Asthma 48, 358–365.

Zhu, Y., Zhao, L., Liu, L., Gao, P., Tian, W., Wang, X., Jin, H., Xu, H., Chen, Q., 2010. Beclin 1 cleavage by caspase-3 inactivates autophagy and promotes apoptosis. Protein Cell 1, 468–477. https://doi.org/10.1007/s13238-010-0048-4.